IOPscience iopscience.iop.org

Home Search Collections Journals About Contact us My IOPscience

Interplay between magnetism and superconductivity in iron-chalcogenide superconductors: crystal growth and characterizations

This article has been downloaded from IOPscience. Please scroll down to see the full text article.

2011 Rep. Prog. Phys. 74 124503

(http://iopscience.iop.org/0034-4885/74/12/124503)

View the table of contents for this issue, or go to the journal homepage for more

Download details:
IP Address: 169.229.32.136
The article was downloaded on 07/10/2011 at 15:55

Please note that terms and conditions apply.

Rep. Prog. Phys. **74** (2011) 124503 (22pp) doi:10.1088/0034-4885/74/12/124503

Interplay between magnetism and superconductivity in iron-chalcogenide superconductors: crystal growth and characterizations

Jinsheng Wen[1,2,3], **Guangyong Xu**[2], **Genda Gu**[2], **J M Tranquada**[2] **and R J Birgeneau**[1,3]

[1] Physics Department, University of California, Berkeley, CA 94720, USA
[2] Condensed Matter Physics and Materials Science Department, Brookhaven National Laboratory, Upton, NY 11973, USA
[3] Materials Science Division, Lawrence Berkeley National Laboratory, Berkeley, CA 94720, USA

E-mail: jinshengwen@berkeley.edu and jtran@bnl.gov

Received 7 April 2011, in final form 9 July 2011
Published 19 September 2011
Online at stacks.iop.org/RoPP/74/124503

Abstract

In this review, we present a summary of results on single crystal growth of two types of iron-chalcogenide superconductors, $Fe_{1+y}Te_{1-x}Se_x$ (11), and $A_xFe_{2-y}Se_2$ (A = K, Rb, Cs, Tl, Tl/K, Tl/Rb), using Bridgman, zone-melting, vapor self-transport and flux techniques. The superconducting and magnetic properties (the latter gained mainly from neutron scattering measurements) of these materials are reviewed to demonstrate the connection between magnetism and superconductivity. It will be shown that for the 11 system, while static magnetic order around the reciprocal lattice position $(0.5, 0)$ competes with superconductivity, spin excitations centered around $(0.5, 0.5)$ are closely coupled to the materials' superconductivity; this is made evident by the strong correlation between the spectral weight around $(0.5, 0.5)$ and the superconducting volume fraction. The observation of a spin resonance below the superconducting temperature, T_c, and the magnetic-field dependence of the resonance emphasize the close interplay between spin excitations and superconductivity, similar to cuprate superconductors. In $A_xFe_{2-y}Se_2$, superconductivity with $T_c \sim 30$ K borders an antiferromagnetic insulating phase; this is closer to the behavior observed in the cuprates but differs from that in other iron-based superconductors.

(Some figures in this article are in colour only in the electronic version)

Contents

1. Introduction 2
2. Crystal growth 2
2.1. Bridgman method 3
2.2. Optical zone-melting technique 5
2.3. Vapor self-transport and flux method 5
2.4. Remaining challenges 5
3. Superconductivity in iron chalcogenides 6
3.1. Superconductivity in the 11 system 6
3.2. Pressure study on the 11 system 7
3.3. Doping with 3d transition metals into $Fe_{1+y}Te_{1-x}Se_x$ 8
3.4. Superconductivity in $A_xFe_{2-y}Se_2$ (A = K, Rb, Cs, Tl, Tl/K, Tl/Rb) 9
3.5. Summary 10
4. Magnetic correlations 10
4.1. Magnetic order 10
4.2. Spin excitations in $Fe_{1+y}Te_{1-x}Se_x$ 12
4.3. Summary 14
5. Conclusions 15
Acknowledgments 15
References 15

 © 2011 IOP Publishing Ltd Printed in the UK & the USA

1. Introduction

A superconducting material can conduct electric current with zero-energy loss due to the absence of electrical resistance below its superconducting transition temperature T_c; such behavior is clearly of great practical use [1]. On the theoretical side, superconductivity was initially understood with the many-body theory developed by Bardeen, Cooper and Schrieffer (BCS theory) [2]; these authors explained the phenomenon of superconductivity on the basis of electron pairs whose interaction is mediated by electron–phonon coupling. In the 1980s, high-temperature superconductivity was discovered in lamellar copper-oxide materials whose T_c can be above liquid-nitrogen temperature [3, 4]. Here, the electron–phonon coupling as proposed in BCS theory is not sufficient to induce superconductivity at such high temperatures [5, 6]. In these cuprate superconducting materials, superconductivity develops from electronically doping an antiferromagnetic Mott insulating phase with carriers [5–9]. It is thus hoped that one may eventually understand the high-T_c superconductivity in terms of the interplay between magnetism and superconductivity.

Research on high-T_c superconductivity turned in a new direction in the year 2008 with the discovery of iron-pnictide superconductors [10, 11]. The initial excitement came with the discovery of superconductivity by Hosono's group in $LaFeAsO_{1-x}F_x$ (labeled 1111, based on the elemental ratios in the chemical formula of the parent material) with $T_c = 26$ K [11], following an earlier report of superconductivity in $LaFePO_{1-x}F_x$ with $T_c \sim 5$ K by the same group [10]. The T_c was soon raised to 43 K, either by replacing La with Sm ($SmFeAsO_{1-x}F_x$) [12], or by applying pressure [13]. Several 1111 superconductors with $T_c > 50$ K have been successively reported [14–17], and the current record is 56 K in $Gd_{1-x}Th_xFeAsO$ [17]. In addition to the 1111 system, four other families of iron-based superconductors have been discovered, typified by $BaFe_2As_2$ (1 2 2) [18–21], LiFeAs (111) [22–27], $Fe_{1+y}Te_{1-x}Se_x$ (11) [28–32] and Sr_2PO_3FePn (21311) [33, 34]. Their crystal structures (figure 1) are all tetragonal at room temperature, but the 122 family crystallizes in the $I4/mmm$ space group, while the space group is $P4/nmm$ for the others [10, 26, 35–38]. One important common feature is that they are all layered structures, as in the cuprates [5–9].

Extensive research has been carried out to study the magnetic correlations. It is now well established for these materials that long-range antiferromagnetic order is suppressed with doping, while superconductivity appears above a certain doping level [36–57]. While there are a few cases where superconductivity appears suddenly after magnetic order disappears [46], it is more commonly found that magnetic order, either short- or long-ranged, coexists in some fashion with superconductivity over a finite range of doping [45, 47–51, 53, 55]. The observations that superconductivity develops concomitantly with the suppression of antiferromagnetic order in many iron-based superconductors [39, 55, 58, 59], a behavior similar to that in cuprates [5–9, 60], suggest that there could also be a similar connection with the superconductivity. Conceptually, the simplest possibility would involve having the magnetic excitations replace phonons in the electron pairing interaction, and in the iron-based superconductors the finite momentum of the antiferromagnetic fluctuations is proposed to facilitate interband pairing [61–67]. Of course, the role of the magnetic correlations could depend on the nature of the magnetism, which continues to be a subject of intense investigation [68–75]. Furthermore, four or five Fe 3d orbitals are involved in the multiple bands that cross the Fermi energy, and excitations among these orbitals have also been proposed as possible contributors to the pairing mechanism [76]. In any case, the magnetic excitations respond strongly to the superconductivity: the low-energy fluctuations are gapped, and the spectral weight moves into a 'resonance' peak above the gap; the resonance peak has been observed in a number of iron-based superconductors [77–85]. Obviously, the iron-based superconductors provide new opportunities to address the long-standing challenge of high-T_c superconductivity, and this has made them some of the most heavily studied materials in condensed matter physics over the past three years. A number of reviews are already available on these superconductors [56, 86–95].

Among the five types of iron-based superconductors, the T_c for the 11 system is the lowest [89]. However, the 11 materials are still of particular interest for a number of reasons: (i) As seen from figure 1, the crystal structure is the simplest, which makes it easier to study them; (ii) 11 system does not contain As, thus making it safer to handle; (iii) Most importantly, high-quality, large-size single crystals can be made available for this system (with $x \leqslant 0.7$), as will be discussed in section 2. This is especially important for neutron scattering experiments because, although neutrons represent a powerful probe of magnetic correlations, the limitations of neutron source strength and scattering cross sections require the use of samples of considerable size ($\gtrsim 1\ cm^3$) in order to obtain reliable data.

More recently, the discovery of superconductivity in a ternary iron-chalcogenide system with the approximate formula $A_xFe_{2-y}Se_2$ (A = K, Rb, Cs, Tl, Tl/K, Tl/Rb), whose highest T_c is ~33 K at ambient pressure, has stimulated considerable interest [96–100]. The structure at high temperature is equivalent to that of the 122 materials, as shown in figure 1 (1 2 2).

The rest of this paper is organized as follows: in section 2, we present the efforts on crystal growth that make many further measurements possible; in section 3, superconductivity in both the 11 and $A_xFe_{2-y}Se_2$ systems is discussed; in section 4, the static and dynamic spin correlations obtained mainly by neutron scattering experiments are presented, followed by the conclusions in section 5.

2. Crystal growth

Fe–Se has a very complicated phase diagram [101]. The superconductivity in this system was found in the β-$Fe_{1+y}Se$, which has a tetragonal structure [28, 102]. A modified phase diagram (figure 2(a)) indicates that the β-phase only exists in

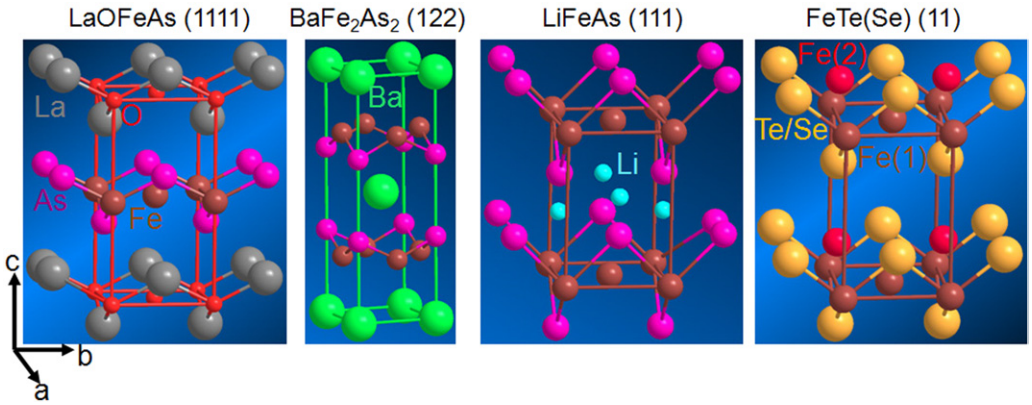


Figure 1. Crystal structures for the 1111, 122, 111 and 11 type iron-based superconductors.

a narrow temperature (300–440 °C) and composition window (Fe : Se = 1.01–1.03) [102]. Because there is no common phase boundary line between the liquid phase region and the $Fe_{1+y}Se$ solid phase region in the Fe–Se phase diagram [101], it is not possible to grow a single crystal of $Fe_{1+y}Se$ directly from Fe–Se liquid. Therefore, methods that rely on growing a crystal directly from a melt cannot be used in this case. Instead, other growth methods, such as vapor self-transport growth [103] and alkali-halide-flux growth [104–106] have been reported.

In contrast, tetragonal $Fe_{1+y}Te$, though not superconducting, is stable in a larger temperature and composition space (figure 2(*b*)), and large single crystals can be grown directly from the melt, with a certain amount of excess Fe [30, 31]. It was quickly found that mixing Se with Te both optimizes T_c (at ambient pressure) and allows melt growth techniques. Indeed, to date, large-size single crystals of $Fe_{1+y}Te_{1-x}Se_x$ with $x \leqslant 0.7$ have been successfully grown using several standard melting techniques, including Bridgman (vertical and horizontal) [30, 31, 55, 85, 108–119] and optical zone-melting [120]. For the newly discovered $A_xFe_{2-y}Se_2$ system, typically the Bridgman method has been employed [96–98, 121–125].

2.1. Bridgman method

In figures 3(*a*) and (*c*) we show the schematics for the vertical and horizontal versions of the Bridgman technique. An example of a synthesis scheme is as follows. To start with, the raw materials (99.999% Te, 99.999% Se and 99.98% Fe) are weighed and mixed with the desired molar ratio, and then sealed into an evacuated, high-purity (99.995%) quartz tube. Since the tube often cracks during the cooling cycle, it is sealed inside a larger evacuated tube. The doubly sealed materials are then put into the furnace vertically (or horizontally) for pre-melting, with the following sequence: ramp to 660 °C in 2 h; hold for 1 h; ramp to 900 °C in 1 h; hold for 1 h; ramp to 1050 °C in 1 h; hold for 3 h; shut down the furnace and cool to room temperature. The reacted materials are then crushed and double-sealed into evacuated quartz tubes for the growth sequence: ramp to 660 °C in 3 h; hold for 1 h; ramp to 900 °C in 2 h; hold for 1 h; ramp to 1000 °C in 1 h; hold for 12 h; cool to 300 °C with a cooling rate of −0.5 or −1 °C h^{-1}; shut down the furnace and cool to room temperature. In the furnace, there

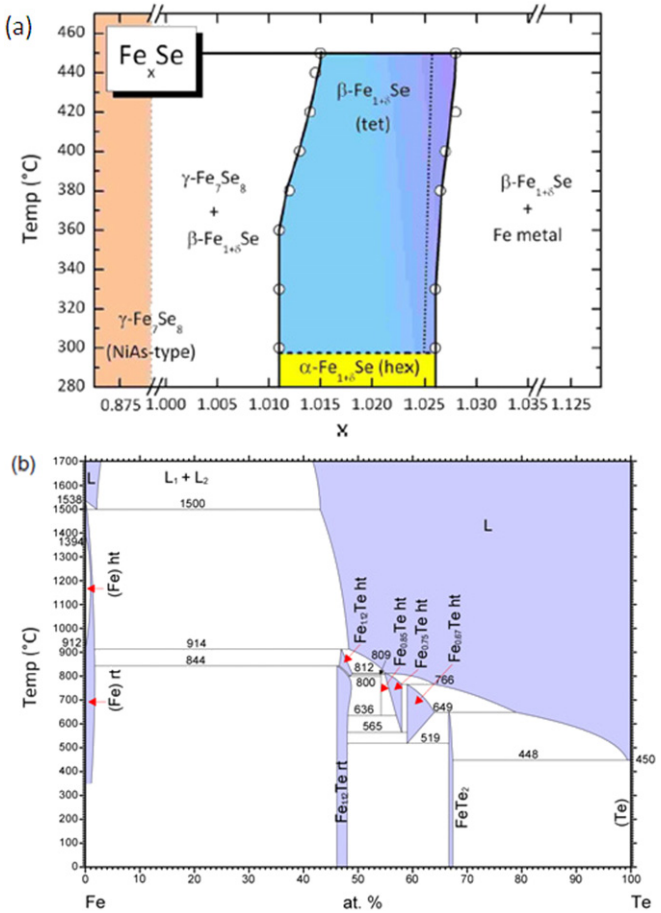


Figure 2. (*a*) Phase diagram for Fe–Se. Reprinted with permission from [102]. Copyright 2009 by the American Physical Society. (*b*) Phase diagram for Fe–Te. Reprinted from [107]. Copyright 1990 ASM International.

should be a small temperature gradient from one end to the other (e.g. at 850 °C, ΔT/distance ≈5 °C cm^{-1}) as shown in figures 3(*a*) and (*c*), which allows directional solidification of the melted liquid. (Some may choose to skip the pre-melting step.) By using this method, large-size (>10 g) high-quality single crystals can be obtained for $Fe_{1+y}Te_{1-x}Se_x$ with $x \leqslant 0.7$. Figures 3(*b*) and (*d*) show some of the crystals grown using vertical and horizontal Bridgman methods. The crystals

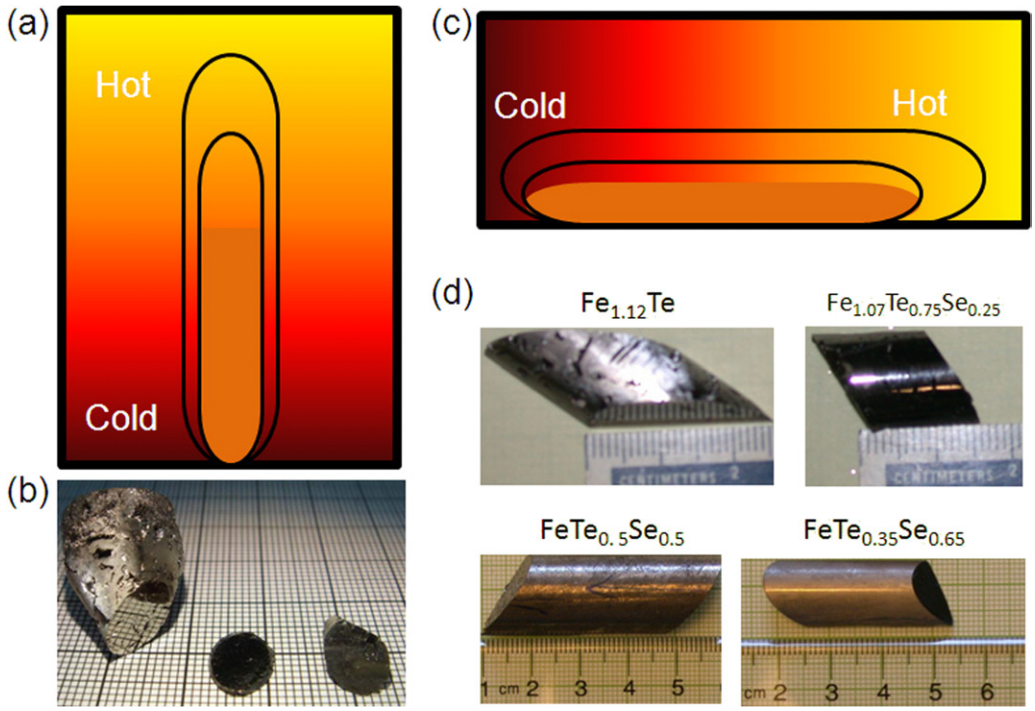


Figure 3. (*a*) Schematic of the vertical Bridgman growth. (*b*) Crystals grown using the method shown in (*a*). Reprinted with permission from [30]. Copyright 2009 by the American Physical Society. (*c*) Horizontal Bridgman growth. (*d*) Crystals grown using the method shown in (*c*) [126].

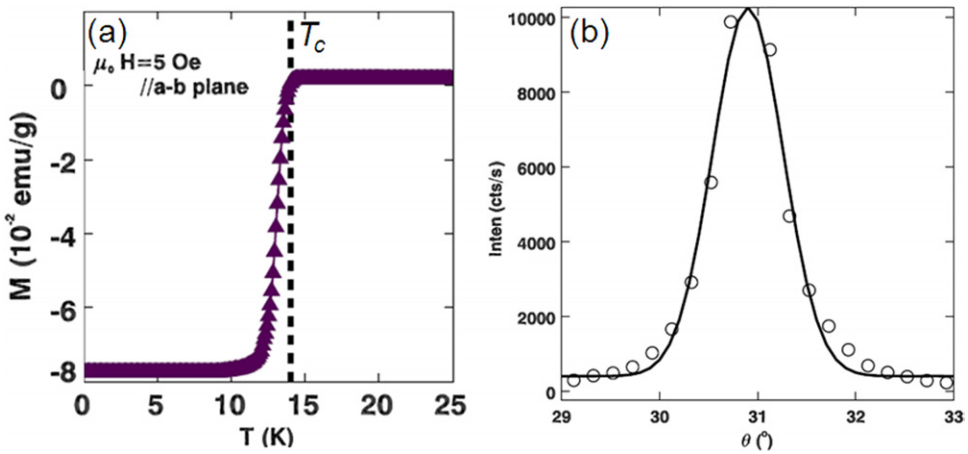


Figure 4. (*a*), (*b*) Magnetization and (110) rocking curve of $FeTe_{0.5}Se_{0.5}$ samples.

can have nice mirror-like cleavage surfaces, corresponding to the *a*–*b* planes; however, in our experience, such crystals have excess Fe ($y > 0$) and a reduced superconducting volume fraction. Crystals with a large superconducting volume fraction (with $y \approx 0$) tend to have a textured cleavage surface associated with slight misorientation of grains, due to strain effects that develop on cooling in the constrained cross section of a quartz tube.

Many measurements such as resistivity, magnetization, x-ray diffraction (XRD) and neutron diffraction have been carried out to characterize such crystals [30, 31, 55, 85, 108–119]. In figure 4 we show the bulk magnetization and rocking curve for $FeTe_{0.5}Se_{0.5}$ samples. The transition width, ΔT_c, is $\sim$1 K (figure 4(*a*)), indicating that the sample is reasonably homogeneous. From neutron diffraction measurements, we obtained a mosaic spread of 0.85° for a 9 g sample (figure 4(*b*)). These demonstrate that high-quality, large-size single crystals of $Fe_{1+y}Te_{1-x}Se_x$ ($x \leqslant 0.7$) can be successfully grown using the Bridgman method.

To grow single crystals of $A_xFe_{2-y}Se_2$, a similar method is used. First, FeSe is prepared as the precursor by reacting Fe and Se in the appropriate ratio at 700 °C for 4 h. The alkali and the precursor FeSe are loaded into an alumina crucible with the nominal composition, which was then sealed into a tube; Wang *et al* [121] have demonstrated the benefits of using an arc-welded Ta tube. The tube is then put into an evacuated quartz tube and sealed. A typical growth sequence is as follows: ramp to 1050 °C in 15 h; hold for 4 h; cool to 750 °C at a rate of -1 to -3 °C h^{-1}; shut down the furnace and cool to room temperature. Large-size single crystals can be obtained using



Figure 5. Single crystal rods of $K_{0.8}Fe_2Se_2$ grown using the vertical Bridgman method [127].

this method, and single crystal rods thus obtained are shown in figure 5. A one-step method using a similar growth procedure but without first reacting Fe and Se as the precursor has also been reported [125].

2.2. Optical zone-melting technique

Yeh *et al* [120] have used the optical zone-melting method to grow $Fe_{1+y}Te_{1-x}Se_x$ single crystals with x ranging from 0 to 0.7. The advantage of this technique is that it offers the possibility of visually examining the locally melted zone, as well as providing convenient control of the growth rate using the image furnace. A schematic of the setup is shown in figure 6(*a*). To grow single crystals, powders of 99.9% Fe, 99.9% Se and 99.999% Te were combined with the desired stoichiometry and mixed in a ball mill for 4 h. The mixed powders were cold pressed into discs under 400 kg cm^{-2} uniaxial pressure, and then sealed into an evacuated quartz tube. The tube was heated at 600 °C for 20 h. The reacted bulk material was reground to fine powder and then sealed into an evacuated quartz tube. The tube was sealed into a second evacuated tube, and then loaded into an optical floating-zone furnace with two 1500 W halogen lamps installed inside the mirrors as infrared radiation sources, as shown in figure 6(*a*). The ampule was rotated at a rate of 20 rpm and moved downward at a rate of 1–2 mm h^{-1}. The as-grown crystals were annealed with the following sequence: ramp to 700–800 °C in 7 h; hold for 48 h; cool to 420 °C in 4 h; hold for 30 h; shut down the furnace and cool to room temperature.

The inset of figure 6(*a*) shows an as-grown crystal for $FeSe_{0.3}Te_{0.7}$, which has an easily cleaved surface perpendicular to the c-axis [120]. As shown in figure 6(*b*), only (0 0 L) peaks were found in the typical XRD pattern on a cleaved surface of the crystal, indicating that the cleaved surface corresponds to the a–b plane. In the inset of figure 6(*b*) it is shown that the crystal has a mosaic as small as 0.092°. The phase purity was examined by x-ray powder diffraction with powder obtained by crushing the crystals. Yeh *et al* [120] found that all diffraction peaks of crystals with $x < 0.7$ belong to the tetragonal phase and no secondary phase was observed. High-resolution transmission electron microscopy (TEM) measurements showed that the diffraction patterns could be well indexed with a tetragonal structure, as shown in the inset of figure 6(*c*) [120].

2.3. Vapor self-transport and flux method

The phase diagram of Fe–Se is such that one cannot grow large crystals of β-FeSe directly from the standard melting methods; Patel *et al* [103] used vapor self-transport as an alternative approach. They began by mixing 99.9% Fe and 99.99% Se powders with the desired molar ratio. The mixture was ground and sealed into an evacuated quartz tube. The material was then heated in a three-zone furnace with the following procedure: (1) heat the material with the temperatures for the three zones set to 700 °C (where the Fe and Se mixture is located), 900 °C and 900 °C, respectively, for 5 days; (2) crystal nucleation is initiated by setting the temperature of all zones to 700 °C, and the temperature held constant for 5 h; (3) the crystals are left growing for 30 days with a temperature setting of 825 °C, 700 °C and 825 °C, respectively; (4) the system is cooled to 400 °C rapidly, and the temperature is kept constant for 10 h; (5) cool to room temperature at a rate of −3 °C min^{-1}. XRD indicated that the dominant phase in the as-grown crystal was superconducting β-$Fe_{1+y}Se$, with a minority of non-superconducting α-FeSe [103].

Another approach is to use an alkali-halide flux. Zhang *et al* [104] made use of a NaCl/KCl flux. First, Fe and Se powders with the desired stoichiometry were reacted to obtain $Fe_{1+y}Se$ polycrystalline samples. This material was mixed with NaCl/KCl flux (ratio 1 : 1), and the combination was ground and sealed in an evacuated quartz tube. The quartz tube was heated to 850 °C. The temperature was maintained at 850 °C for 2 h before cooling to 600 °C at a rate of −3 °C h^{-1}. Finally, the furnace was cooled rapidly to room temperature. The crystals were separated from the flux by dissolving the NaCl/KCl flux in deionized water. There is also a report of using KCl (KBr) as the flux [106].

Hu *et al* [105] have recently demonstrated an improved method, using a flux of LiCl/CsCl. Refinement of synchrotron XRD data yielded a stoichiometry of $Fe_{1.00(2)}Se_{1.00(3)}$.

2.4. Remaining challenges

As described above, it has been demonstrated that large crystals of $Fe_{1+y}Te_{1-x}Se_x$ with $x \leqslant 0.7$ can be grown from the melt; however, challenges remain in obtaining homogeneous samples [128, 129]. Hu *et al* [129] performed scanning transmission electron microscopy (STEM) and electron energy loss spectroscopy (EELS) measurements on a series of as-grown $Fe_{1+y}Te_{1-x}Se_x$ crystals. They found that all these samples showed nanoscale phase separation and chemical inhomogeneity of the Te/Se content. They attributed this to the presence of a miscibility gap in the phase diagram. The same conclusion was reached in an extended x-ray absorption fine-structure (EXAFS) study on $Fe_{1+y}Te_{1-x}Se_x$, where it was observed that the local structure differed from the average [128]. Scanning tunneling microscopy/spectroscopy (STM/STS) measurements on a $FeTe_{0.55}Se_{0.45}$ sample also showed that there were Te- and Se-rich regions, whereas the averaged Te and Se contents were still 0.55 and 0.45, respectively [130]. The sample inhomogeneity may account for the broad transitions in these materials [91, 120]. One way to improve crystals is to use a smaller cooling rate during the growth. For example, from our own experience, using a −1 °C h^{-1} cooling rate yields better crystals than using −3 °C h^{-1}. Annealing the as-grown crystals can also

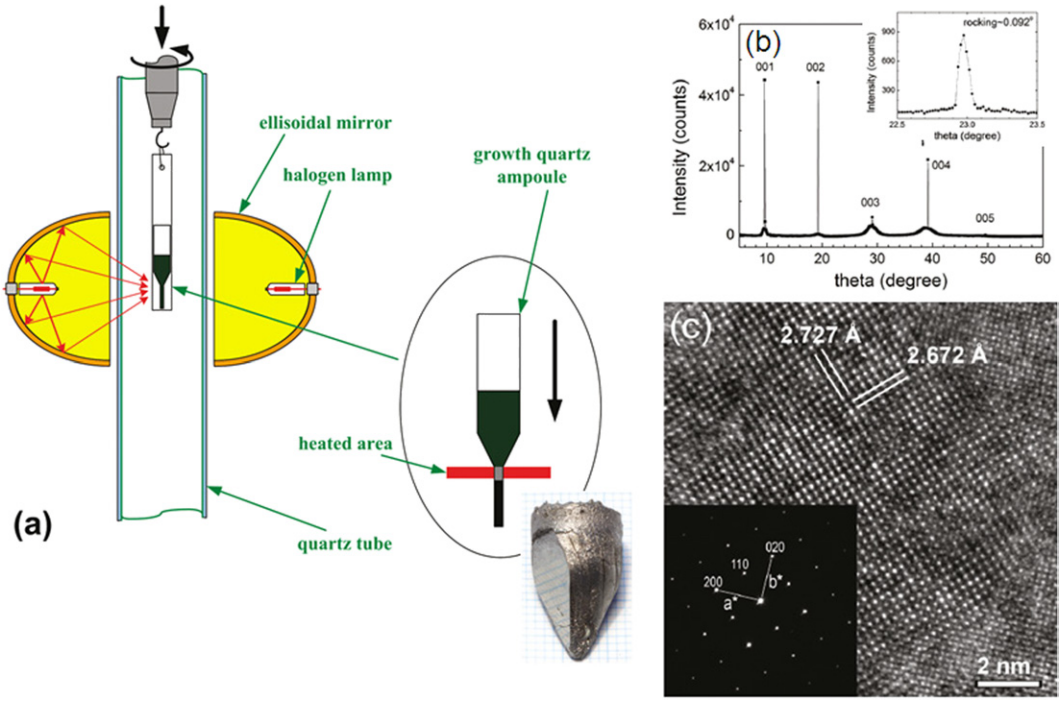


Figure 6. (*a*) Schematic diagram of apparatus setup of the optical zone-melting method. The inset shows an as-grown $FeTe_{0.7}Se_{0.3}$ single crystal on a 1 mm grid. The shiny surface is the *a*–*b* plane. (*b*) XRD pattern for an $FeSe_{0.3}Te_{0.7}$ crystal. Miller indices for the tetragonal-PbO structure are shown. The inset shows the rocking curve for the (101) peak. (*c*) High-resolution TEM image of an $FeSe_{0.3}Te_{0.7}$ crystal and the electron diffraction indexed with a tetragonal lattice. Reprinted with permission from [120]. Copyright 2009 American Chemical Society.

be useful [57, 110, 117, 120]. Vacuum annealing can make the Se/Te distribution more homogeneous, thus improving the superconducting volume fraction [110, 117]. Alternatively, it has been reported that annealing in air reduces the amount of excess iron [57], which can be important for observing bulk superconductivity in samples with large Te concentrations. Annealing in oxygen has been used to induce bulk superconductivity in the sulfide version, $Fe_{1+y}Te_{1-x}S_x$, at small x [108]. It is more challenging to grow crystals of $Fe_{1+y}Te_{1-x}Se_x$ with $x > 0.7$ [120]. So far, large crystals (on the order of 1 g) have not yet been reported in this range. Even for small crystals or polycrystalline samples of $Fe_{1+y}Se$, impurity phases such as α-FeSe, Fe_7Se_8, Fe_3O_4 and Fe are often found [103, 105], because of the complex phase diagram, as shown in figure 2(*a*) [101, 102]. Nevertheless, a recent study has reported the growth of phase-pure and stoichiometric crystals of superconducting FeSe [105].

The major obstacle that limits the understanding of the intrinsic properties of $A_xFe_{2-y}Se_2$ is the difficulty in preparing phase-pure superconducting samples. An initial TEM study on a superconducting sample of nominal composition $KFe_{2-y}Se_2$ ($0.2 \leqslant y \leqslant 0.3$) clearly demonstrates that there is nanoscale phase separation along the *c*-axis—in some regions, there is Fe-vacancy ordering, while in others the vacancies are disordered [131]. In a recent angle-resolved photoemission spectroscopy (ARPES) study, a variety of results were interpreted in terms of the coexistence of different phases separated mesoscopically [132]. More effort on this system will be necessary in order to achieve predictable synthesis of single-phase samples.

3. Superconductivity in iron chalcogenides

3.1. Superconductivity in the 11 system

Superconductivity in the iron chalcogenides was first discovered in $Fe_{1+y}Se$, with zero resistance at $T = 8$ K, as shown in figure 7 [28]. The upper critical field at zero temperature, $\mu_0 H_{c2}(0)$, was estimated to be 16.3 T [28]. The composition of the superconducting phase was initially reported to be $FeSe_{0.88}$ by Hsu *et al* [28], and a similar composition, $FeSe_{0.92}$, was identified by Margadonna *et al* [133]; however, these powder samples showed a significant fraction of secondary phases in diffraction measurements. McQueen *et al* [102] followed this work with a careful study of synthesis conditions and composition. They showed that synthesis from powders generally leads to problems with oxygen contamination, resulting in an overestimate of the Fe content in the sample. By using large pieces of Fe and Se as starting materials, they found that the stable composition range of $Fe_{1+y}Se$ is $0.01 \leqslant y \leqslant 0.03$ (consistent with a much earlier work on the phase diagram [101]), with $T_c = 8.5$ K at $y = 0.01$ and dropping to zero at 0.03. Synchrotron XRD indicated single-phase samples. As a further test, Pomjakushina *et al* [134] prepared a series of samples with different initial compositions, and analyzed the composition by Rietveld refinement of neutron powder diffraction data, obtaining $FeSe_{0.975}$ (or $Fe_{1.025}Se$) for the superconducting phase in these multiphase samples, close to stoichiometry. Finally, there is the impurity-free single crystal of Hu *et al* [105] that has been shown to be stoichiometric. It seems reasonable to conclude that the superconducting composition

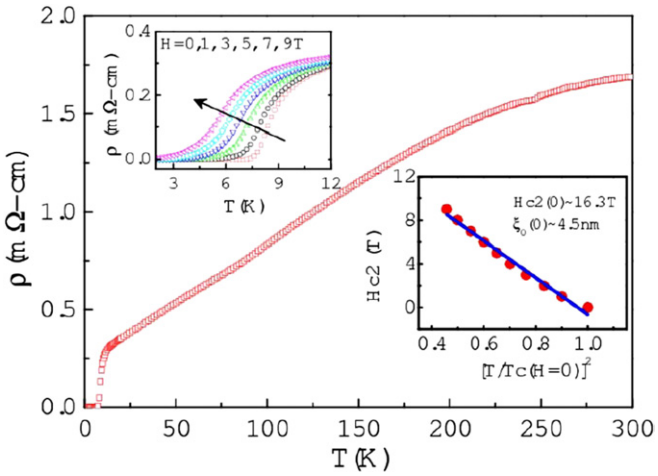


Figure 7. Temperature dependence of electrical resistivity (ρ) of $Fe_{1.14}Se$. The left inset shows resistivity versus temperature under different field strengths below 12 K. The right inset shows the temperature dependence of the upper critical field. Reprinted with permission from [28]. Copyright 2008 National Academy of Sciences of the USA.

is close to stoichiometry. To establish convincingly the nature of any defects (Fe interstitials, Se vacancies, etc), one would need to test for diffuse scattering from a single crystal. Such measurements on $Fe_{1+y}Te$ have revealed a clear signature of atomic displacements associated with Fe interstitials [135].

At room temperature, $Fe_{1+y}Se$ has a tetragonal PbO-type structure belonging to the $P4/nmm$ space group as shown in figure 1 (1 1). It has an iron-based planar sublattice equivalent to that of the iron pnictides [10, 11]. On cooling below ~90 K, there is a structural transition to an orthorhombic phase (space group $Cmma$) [133, 134, 136], resulting in a subtle distortion of the $FeSe_4$ tetrahedra. The transition temperature is observed to be sensitive to composition [136].

Systematic results for the in-plane electrical resistivity of $FeTe_xSe_{1-x}$ are shown in figure 8(a) [30]. $Fe_{1+y}Te$ is not superconducting; instead, it exhibits coincident magnetic and structural transitions at ~65 K [53, 137–139]. This behavior is similar to that of the undoped phases of the 1111 and 122 materials [37, 39–57], and it is therefore often referred to as the parent compound for the 11 system [32, 137, 138, 140, 141]. By replacing Te with Se, the structural transition temperature is gradually suppressed [139]. With 6% Se doping, a trace of superconductivity starts to appear, and coexists with the antiferromagnetic order [53]. With increasing Se content, the superconducting volume fraction improves, and T_c also becomes optimized for $x \sim 0.5$ [29, 30, 32]. Superconductivity extends all of the way to $x = 1$ in $Fe_{1+y}Se$, as discussed above.

Other combinations of chalcogenides are also possible. For example, one can substitute S for Se in $Fe_{1+y}Se_{1-z}S_z$. For $z = 0.2$, T_c is increased slightly, to 10 K [142]. The T_c increase is accompanied by suppression of the tetragonal-to-orthorhombic transition temperature, with the transition already absent at $z = 0.1$ [142]. For $z > 0.2$, T_c gradually decreases, with no superconductivity observed for 0.4 S [142]. Doping S into the parent compound $Fe_{1+y}Te$ can also induce superconductivity [108, 119, 140], while suppressing the magnetic and structural transitions. The highest T_c in the $Fe_{1+y}Te_{1-z}S_z$ system is 10 K in $FeTe_{0.8}S_{0.2}$ [140].

Figure 8(b) shows the magnetic susceptibility and resistivity of the optimally doped sample, $FeTe_{0.5}Se_{0.5}$ [30]. It has a T_c of 14 K, highest in the 11 system at ambient pressure, with a superconducting volume fraction close to 100% [30, 85]. One thing to note is that in some of the thin film samples, an enhancement of T_c was observed [143, 144] (which may be related to strain effects, as pressure can enhance T_c; see section 3.2), while in other cases the opposite effect has been reported [145, 146]. For the optimally doped compound, the estimated $\mu_0 H_{c2}(0)$ is $\gtrsim$70 T [85], which makes it comparable to other iron-based and cuprate superconductors [143, 147, 148]. Similar to the iron-pnictide superconductors, the anisotropy for the 11 system is small. For instance, in $Fe_{1.03}Te_{0.7}Se_{0.3}$, the anisotropy coefficient γ (ratio of $\mu_0 H_{c2}$ measured in and out of plane) is less than 2 [31].

A number of groups have reported similar phase diagrams for $Fe_{1+y}Te_{1-x}Se_x$ [52–57]; one version, obtained from magnetization measurements, is shown in figure 9. At first glance, this phase diagram is similar to those of the cuprate [5–9] and iron-pnictide superconductors [37, 39–54, 56, 57]. The undoped compound is an antiferromagnet; with doping, the transition temperature is reduced, and superconductivity appears above 0.1 Se doping (see [52–54]), with T_c versus doping x having a dome shape. However, there are several important differences which need to be pointed out. (i) Unlike most other high-T_c superconductors, where 'doping' refers to substitution of elements with a different valence, here the replacement of Te with Se is isovalent. The positive Hall coefficient in $Fe_{1.03}Te_{0.7}Se_{0.3}$ indicates that hole carriers are dominant with Se doping [31]. (ii) Superconductivity survives to $x = 1$, unlike most other systems where superconductivity disappears with carrier doping above a certain value [89]. (iii) The material's properties can be tuned not only by doping with Se, but also by adjusting the amount of excess Fe. For example, a number of studies of $Fe_{1+y}Te_{1-x}Se_x$ with $x \lesssim 0.5$ have shown that the presence of Fe interstitials correlates with a reduction in superconducting volume fraction [109, 115, 149–151]. Without Se, it appears difficult to reduce Fe content below $y = 0.05$, but the minimum interstitial density decreases as Se is added [139]. The relationship between excess Fe and the magnetic correlations will be discussed in section 4.

3.2. *Pressure study on the 11 system*

In figure 10 we plot the pressure dependence of T_c for four samples. For $Fe_{1+y}Se$, there is a strong pressure dependence [152–155]. Applying a pressure of 1.48 GPa raises T_c to 27 K and $\mu_0 H_{c2}(0)$ to 72 T [156]. With a further increase in pressure, T_c appears to have a maximum of 37 K for pressures above 4 GPa [152–154]. While T_c increases with pressure, the superconducting volume fraction is reported to decrease rapidly for pressure (P) > 1.5 GPa, suggesting significant inhomogeneity [157]. Margadonna *et al* [153] also found that the T_c–P curve coincides with anomalies in the pressure evolution of the interlayer spacing, suggesting an intimate relationship between structure and superconductivity.

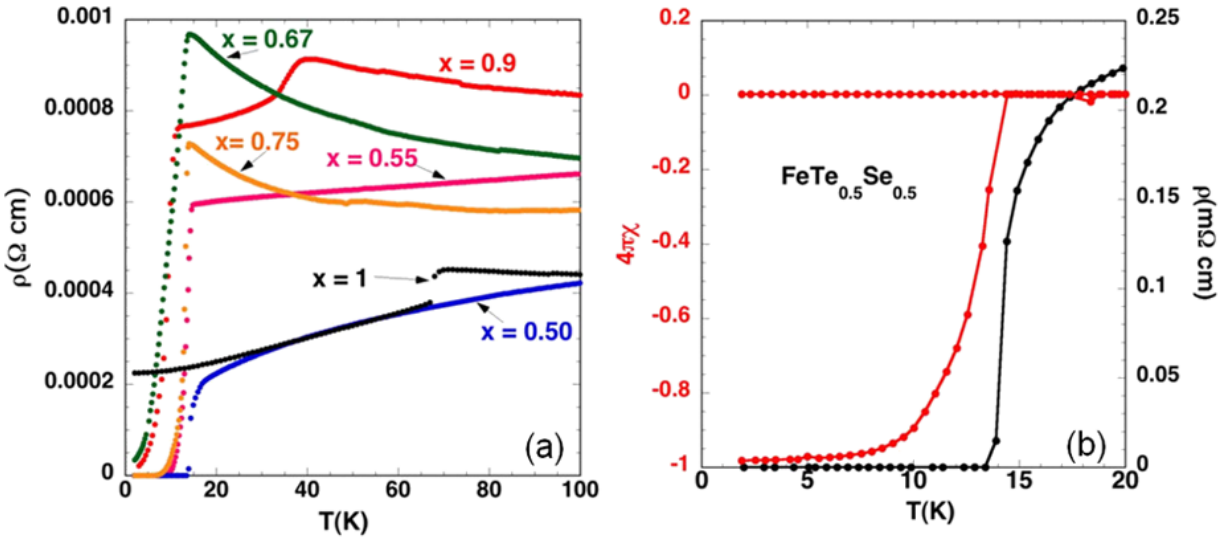


Figure 8. (*a*) In-plane electrical resistivity ρ as a function of temperature for $FeTe_xSe_{1-x}$. (*b*) Magnetic susceptibility of a $FeTe_{0.5}Se_{0.5}$ crystal measured with $\mu_0 H = 20$ Oe using zero-field cooling and field-cooling protocols. The resistivity data from the same sample are also shown on the right axis. Reprinted with permission from [30]. Copyright 2008 by the American Physical Society.

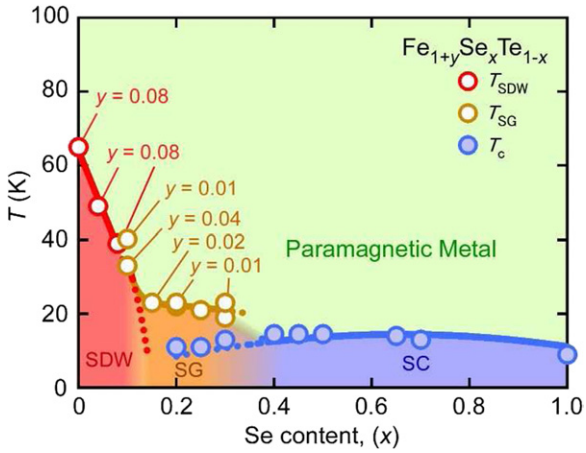


Figure 9. Phase diagram of $Fe_{1+y}Te_{1-x}Se_x$ with $y = 0$ as a function of x and T, constructed from single crystal bulk magnetization data. The nominal Fe content is $y = 0$, unless it is specified. SDW, SG and SC stand for long-range antiferromagnetic, spin-glass and superconducting order, respectively. Reprinted from [55]. Copyright 2010 Physical Society of Japan.

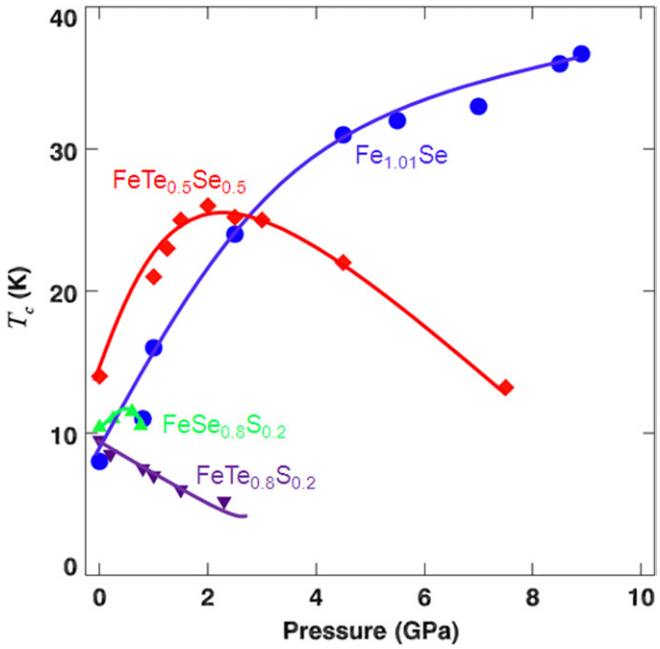


Figure 10. Pressure dependence of the T_c for $Fe_{1.01}Se$, [152] $FeTe_{0.5}Se_{0.5}$, [158] $FeSe_{0.8}S_{0.2}$, [159] and $FeTe_{0.8}S_{0.2}$ [160]

In the compound with mixed Se and Te, the pressure dependence of T_c is similar to that in $Fe_{1+y}Se$, though less dramatic [158, 159, 161]. In $FeTe_{0.5}Se_{0.5}$, the T_c onset increases rapidly from 13.5 to 26.2 K upon application of a pressure of 2 GPa [158]. Above 2 GPa, T_c decreases linearly, and a metallic (non-superconducting) ground state is observed at 14 GPa [158]. In other Se-doped samples, e.g. $FeTe_{0.43}Se_{0.57}$ and $FeTe_{0.75}Se_{0.25}$, the pressure effects are reported to be smaller [56, 159, 161].

For $FeSe_{0.8}S_{0.2}$, a study with pressure up to 0.76 GPa shows only a weak effect on T_c, with an indication of a decline in T_c at higher pressures [159]. Contrary to the pressure enhancement of T_c discussed so far, application of pressure to $Fe_{1+y}Te_{1-x}S_x$ causes T_c to decrease monotonically, as shown in figure 10 [160]. One might guess that applying pressure to the parent compound of the 11 system, $Fe_{1+y}Te$, could make it superconducting; however, superconductivity was not observed in $Fe_{1.09}Te$ with hydrostatic pressure up to 2.5 GPa [162], although the structural transition temperature was reduced [162], and the lattice collapsed [163]. In contrast, superconductivity with T_c up to 13 K has indeed been reported for thin film samples of FeTe under tensile stress [164].

3.3. Doping with 3d transition metals into $Fe_{1+y}Te_{1-x}Se_x$

One can also change the properties of the 11 system by doping with 3d transition metals (Mn, Co, Ni, Cu, etc). There are several initial studies on $Fe_{1+y}Se$ [91, 165–167]. Thomas *et al* [165] have found that 2.5% Co reduces T_c to below 4 K, and

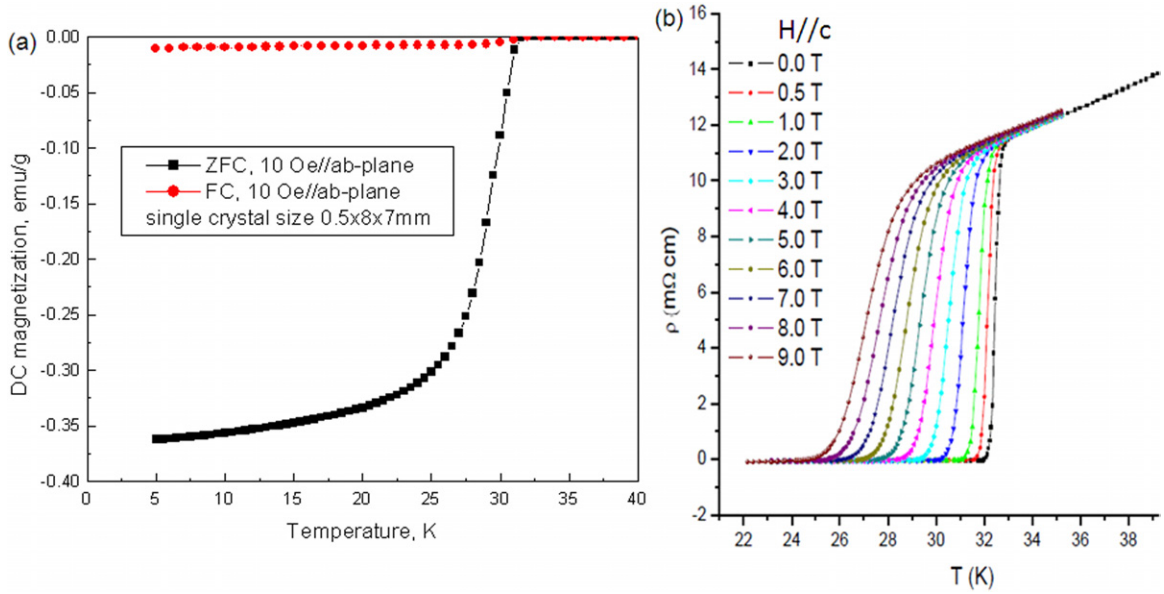


Figure 11. (*a*) Temperature dependence of the magnetization for a $K_{0.8}Fe_2Se_2$ single crystal. (*b*) Resistivity measured in the *a*–*b* plane with field applied along the *c*-axis [127].

no superconductivity is observed for Co doping at and above 5%, though the system is still metallic with 20% Co [142]. Cu seems to have a larger effect in reducing T_c. As little as 1.5% Cu substitution results in the absence of a diamagnetic response [166]. More interestingly, with increased Cu doping (4%), the system evolves into an insulator [166, 167]. Analysis of the temperature dependence of the resistivity suggests that the sample with 10% Cu doping is a Mott insulator [167]. This result has interesting implications for the nature of electronic correlations in the iron chalcogenides. Ni doping is also found to suppress T_c [142, 168], but does not drive the system to an insulating state for Ni concentrations up to 20% [142]. Mn substitution has little effect on T_c, and the system remains metallic and superconducting with Mn doping up to 5.5% [167].

Similar studies have been carried out in $Fe_{1+y}Te_{1-x}Se_x$ with $x = 0.35$ [169] and 0.5 [170]. It is found that Co, Ni and Cu all suppress T_c [169] and a metal-to-insulator transition is induced with both Co and Ni doping in $FeTe_{0.5}Se_{0.5}$ samples [170]. There is also a report on Ni-doped $Fe_{1.1}Te$, which reveals that the lattice constants decrease with increasing Ni content [171].

3.4. Superconductivity in $A_xFe_{2-y}Se_2$ (A = K, Rb, Cs, Tl, Tl/K, Tl/Rb)

At the end of the year 2010, Guo *et al* [96] reported that superconductivity with T_c above 30 K had been achieved in a ternary iron chalcogenide, $K_{0.8}Fe_2Se_2$ by intercalating the metal K in between FeSe layers. In figure 11 we show results for the temperature dependence of the magnetization and in-plane resistivity for a $K_{0.8}Fe_2Se_2$ single crystal [127]. The T_c was ~32.5 K, the highest among all iron-chalcogenide superconductors at ambient pressure. This new superconductor with such a high T_c soon ignited another wave of intense activity. To date, in addition to $K_xFe_{2-y}Se_2$ [96, 97, 122, 172–178], superconductivity has been found in a series of compounds with the formula $A_xFe_{2-y}Se_2$ where A = Rb, Cs, Tl, Tl/K or Tl/Rb [98–100, 123, 124, 179–184], and the highest T_c achieved so far is ~33 K. By substituting S ($K_xFe_{2-y}Se_{2-z}S_z$), T_c does not decrease for z up to 0.4 [185, 186], but with $z = 1.6$, superconductivity is completely suppressed [185]. In contrast, Co doping in $K_{0.8}Fe_2Se_2$ has a very strong effect. With 0.5% Co, T_c is reduced to 5 K [187]. A number of the newly discovered $A_xFe_{2-y}Se_2$ superconductors and their T_cs are summarized in table 1, from which one can see that the T_c is not very sensitive to the stoichiometry, except for the Co-doped sample.

There have been some pressure studies on these systems. In a $K_xFe_2Se_2$ sample, which had a T_c of 32.6 K, T_c decreased with increasing pressure, while in a sample with a T_c of 31.1 K, a dome-shaped T_c–P curve was observed, with a maximum T_c of 32.7 K at 0.48 GPa [192]. A similar dome shape was observed for $Cs_xFe_2Se_2$, with T_c maximized to 31.1 K at $P = 0.82$ GPa, compared with 30 K at ambient pressure [192]. In a sample with nominal composition of $K_{0.8}Fe_2Se_2$, which had a T_c of 33 K, it was found that, although the onset T_c increased with pressure, the temperature where the resistivity reached zero decreased [197]. In all of the samples studied, the large normal-state resistance was significantly reduced by pressure [181, 192, 197, 198]. In $Cs_{0.8}Fe_2Se_2$, the resistance decreased by two orders of magnitude, concomitant with a sudden T_c reduction at ~8 GPa [181].

In the normal state of these materials, the resistivity–temperature curve exhibits a very pronounced hump [96], which is believed to be irrelevant to superconductivity [121, 180, 192]. However, in $K_{0.8}Fe_{1.7}Se_2$, Guo *et al* [198] found an interesting correlation between superconductivity and the hump: with increasing pressure, the magnitude of the hump went down as T_c did, and the hump disappeared at $P = 9.2$ GPa, coinciding with the complete suppression of the

Table 1. Summary of T_c for the newly discovered $A_xFe_{2-y}Se_2$ superconductors.

Material	T_c (K)	Material	T_c (K)
$K_{0.8}Fe_2Se_2$ [96, 97, 122, 175, 180, 178]	30–33	$K_{0.8}Fe_2Se_{0.8}S_{1.2}$ [185]	18.2
$K_{0.8}Fe_{1.6}Se_2$ [188]	32	$K_{0.8}Fe_{1.995}Co_{0.005}Se_2$ [187]	5
$K_{0.8}Fe_{1.76}Se_2$ [177]	32	$Rb_{0.83(2)}Fe_{1.70(1)}Se_2$ [179]	31.5
$K_{0.65}Fe_{1.41}Se_2$ [189]	32	$Rb_{0.8}Fe_2Se_2$ [190, 180]	32
$K_{0.85}Fe_{1.83}Se_{2.09}$ [191]	30	$Rb_{0.88}Fe_{1.81}Se_2$ [98]	31.5
$K_{0.85}Fe_2Se_{1.8}$ [192]	32.6	$Cs_{0.86}Fe_{1.66}Se_2$ [192, 123, 180]	30
$K_{0.86}Fe_2Se_{1.82}$ [192, 123]	31.1	$Cs_{0.83(2)}Fe_{1.71(1)}Se_{1.96}$ [182]	28.5
$K_{0.7}Fe_{1.8}Se_2$ [176]	28	$Cs_{0.8}Fe_2Se_2$ [181]	32
$K_{0.86}Fe_{1.73}Se_2$ [174]	25	$TlFe_{1.7}Se_2$ [124]	22.8
$K_{0.86}Fe_{1.84}Se_2$ [173]	30	$Tl_{0.58}K_{0.42}Fe_{1.72}Se_2$ [100, 193]	32
$K_{0.83(1)}Fe_{1.66(1)}Se_2$ [179]	29.5	$Tl_{0.64}K_{0.36}Fe_{1.83}Se_2$ [124]	31
$K_{0.8}Fe_{1.7}SeS$ [194]	25	$Tl_{0.63}K_{0.37}Fe_{1.78}Se_2$ [195]	29
$K_{0.8}Fe_2Se_{1.4}S_{0.4}$ [186]	32.8	$Tl_{0.47}Rb_{0.34}Fe_{1.63}Se_2$ [196]	33
$K_{0.8}Fe_2Se_{1.6}S_{0.4}$ [185]	33.2	$Tl_{0.58}Rb_{0.42}Fe_{1.72}Se_2$ [100]	32
$K_{0.8}Fe_2Se_{1.2}S_{0.8}$ [185]	24.6	$Tl_{0.4}Rb_{0.4}Fe_{2-y}Se_2$ [183]	31.8

superconductivity. By normalizing the resistance to the room-temperature value, Seyfarth *et al* [181] found that the hump still existed at $P = 9$ GPa, at which pressure the sample was not superconducting; based on this, they concluded that the hump was not related to the superconductivity.

These newly discovered superconductors are particularly interesting and fundamentally important in part due to their electronic structures. First-principles calculations have shown that the band structure in this new system is quite different from that of other iron-based superconductors [199–204]. In particular, the band near the Brillouin zone center Γ point sinks well below the Fermi level [199–204]. Experimentally, this prediction has been verified by several initial ARPES studies, which show that there is no hole pocket near the Γ point [205, 206]. Instead, there are electron pockets near both the Γ and M (Brillouin zone corner) points [193, 195, 207]. Although this result does not rule out the possibility that interband scattering between the electron pockets at Γ and M could be important to the superconductivity [208], the sign-changed $s_\pm$ pairing symmetry which has been suggested in other iron-based superconductors is not likely to apply here [61, 62, 209]. Several alternatives, including d-wave [208, 210], s-wave [211, 212] and s_{++}-wave [213] superconductivity have been proposed theoretically. A number of ARPES [193, 195, 205–207], nuclear magnetic resonance (NMR) [175, 178, 214] and specific heat measurements [172] have been carried out and all of them indicate that the gap is nodeless.

Another interesting feature which distinguishes the $A_xFe_{2-y}Se_2$ superconductors from other iron-based superconductors is that their superconductivity is in close vicinity to an insulating state, similar to the case of cuprate superconductors [5–9], but not to that of other iron-based superconductors [93]. Interestingly, it is reported that the insulating $K_xFe_{2-y}Se$ sample becomes superconducting by annealing and quenching, and after a few days at room temperature, it is insulating again, showing that the insulating and superconducting states are reversible [215]. Based on these observations, it is suggested that disordering of Fe vacancies plays a key role in rendering the superconductivity [215]. The experimentally observed insulating ground state [124, 180, 185, 194, 216] has stimulated several theoretical calculations [199, 200, 217]. Two possible origins of the insulating behavior have been proposed which are to be verified experimentally: the system might be a Mott insulator [194, 204, 217, 218] (the Mott behavior may have a complex origin where both Fe vacancies and 3d electron–electron correlations play roles as suggested in [204]), or it might be a band insulator resulting from the electronic structure reconstruction due to ordered Fe vacancies [199, 200].

3.5. Summary

To summarize this section, it is found that the parent compound for the 11 system, $Fe_{1+y}Te$, is non-superconducting, and superconductivity is achieved by replacing Te with Se or S. The optimal superconductivity with T_c of 14 K is found to be in samples with $y = 0$ and $x \approx 0.5$. $Fe_{1+y}Se$ is where superconductivity was initially discovered for the 11 system; it has a T_c of 8 K. The T_c increases to ∼37 K upon application of hydrostatic pressure. The superconductivity seems to be vulnerable to doping with 3*d* transition metals, which can tune the system to a (possibly Mott) insulating regime. More recently, a series of ternary iron-chalcogenide compounds with the chemical formula $A_xFe_{2-y}Se$ were found to be superconducting with T_c up to 33 K, the highest among all Fe–Se-based superconductors at ambient pressure.

4. Magnetic correlations

4.1. Magnetic order

4.1.1. $Fe_{1+y}Te_{1-x}Se_x$ system. The magnetic order in $Fe_{1+y}Te_{1-x}Se_x$ has attracted considerable attention because of its rich physics. An initial band-structure calculation predicted that the Fermi-surface topology in this system should be similar to that of the iron pnictides [219]; this has been confirmed by ARPES measurements [220, 221]. From the Fermi-surface-nesting picture [219], one would expect that this system would have collinear (C-type) spin-density-wave (SDW) order with an in-plane wave vector (0.5, 0.5), assuming a unit cell containing two irons as shown in figure 12(*b*). However, several decades ago, Fruchart *et al* [222] determined that the magnetic ordering vector is

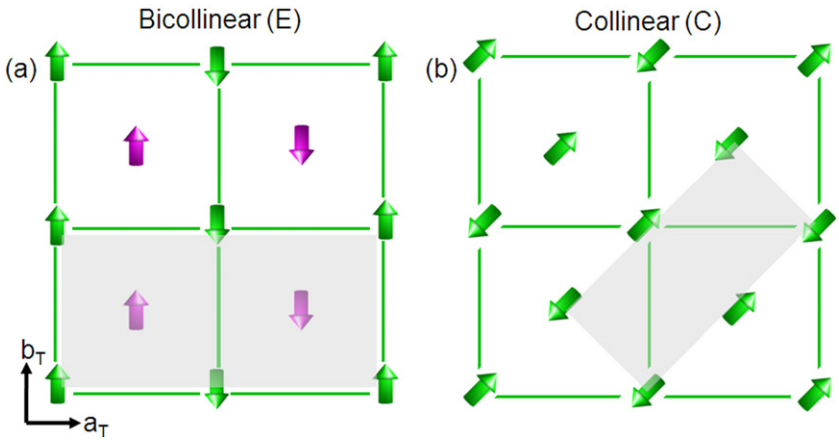


Figure 12. (*a*) Schematic for the bicollinear (E-type) in-plane spin structure in tetragonal notation of the 11 compound. (*b*) Collinear (C-type) magnetic structure for iron pnictides. Shadow represents the magnetic unit cell.

$(0.5, 0)$ in $Fe_{1.125}Te$. This result has been confirmed by Bao *et al* [137] in $Fe_{1.075}Te$, and by Li *et al* [138] in $Fe_{1.068}Te$; each of these has a bicollinear (E-type) spin structure as shown in figure 12(*a*). Even more surprising is the fact that ARPES measurements have observed no SDW nesting instability along $(0.5, 0)$, although there is a weak hole pocket around the X point [220, 223]. Clearly, a simple nesting mechanism cannot account for these experimental results. More recent first-principles calculations have identified the role of local moments and the importance of Hund's exchange coupling, and have provided better agreement with the experimental observations [42, 74, 224–228].

The magnetic order in $Fe_{1+y}Te$ is long-ranged, with a maximum moment size of $\sim$2.5 μ_B/Fe for $y = 0.05$ [139]; the moment size decreases for larger y [137, 138, 222]. The moment size is significant compared with that in iron-pnictide antiferromagnets, but it is small compared with the effective moment estimated from the magnetic susceptibility in the paramagnetic phase [229]. The moment is found to be aligned mostly along the *b*-axis as shown in figure 12(*a*) [137–139]. Bao *et al* [137] have shown that the order can be commensurate or incommensurate depending upon the amount of excess Fe—with more Fe, the incommensurability is larger. Upon doping with Se, the order is suppressed, with a reduced ordering temperature (from 65 to $\lesssim$30 K with 0.1 Se) [55], reduced size of the ordered magnetic moment (from 2.1 to 0.27μ_B/Fe) [53], and shorter correlation length (the magnetic peak is resolution limited in the parent compound, while with 0.25 Se doping, the order is short-ranged with a correlation length of $\sim$4 Å [112, 137]). For Se content above 0.15, there is a phase where spin-glass order and superconductivity coexist [52, 53, 55, 112, 139]. In two single crystal samples, $Fe_{1.07}Te_{0.75}Se_{0.25}$ and $FeTe_{0.7}Se_{0.3}$, both exhibiting short-range incommensurate order below 40 K, it is found that with increasing excess Fe, the incommensurability is larger, similar to the case in the parent compound [112, 137]. In $FeTe_{0.7}Se_{0.3}$, which has more Se and less Fe than the $Fe_{1.07}Te_{0.75}Se_{0.25}$ sample, the spin-glass order is depressed, with weaker peak intensity and shorter correlation length, while superconductivity is enhanced, with higher T_c and superconducting volume fraction [112]. Interestingly, a magnetic peak is only observed on one side of the commensurate wave vector $(0.5, 0)$, (i.e. $(0.5\text{-}\delta, 0)$ and not $(0.5\pm\delta, 0)$ with δ being the incommensurability); this is likely a result of an imbalance of ferromagnetic/antiferromagnetic correlations between neighboring spins [112]. (A closely related picture of spin clusters is indicated by a recent study of $Fe_{1.1}Te$ [229].) With further increase in the Se concentration, the superconductivity optimizes with $x \approx 0.5$, and no static magnetic order is observed (for $y \sim 0$) [52, 53, 85].

Next, we turn to the intriguing case of superconducting $Fe_{1+y}Se$. Although this system exhibits a symmetry-lowering structural transition on cooling through $\sim$90 K [133, 134, 136], measurements with local probes such as Mössbauer spectroscopy [102, 136] and ^{77}Se NMR [230] indicate the absence of static magnetic order. This is in sharp contrast with the case of $Fe_{1+y}Te$; nevertheless, NMR measurements indicate that spin fluctuations increase on cooling toward T_c [230]. In studies of a sample that showed an increase in T_c to 37 K under pressure, Mössbauer measurements indicated the absence of magnetic order up to $\sim$30 GPa [152]. NMR measurements on the same material found that spin fluctuations are enhanced under pressure, along with the superconductivity [230]. In contrast, Bendele *et al* [231] reported evidence for short-range magnetic order for $P \gtrsim 0.8$ GPa based on muon-spin rotation (μSR) measurements; however, this sample showed a much more modest impact of pressure on the superconductivity, with a maximum T_c of 13 K at 0.7 GPa. Mössbauer studies have shown that doping Cu into $Fe_{1+y}Se$ induces a local magnetic moment, with the size of the moment increasing with Cu doping while superconductivity is suppressed [166]. Spin-glass behavior has been inferred from magnetization measurements on these Cu-doped samples [166].

The magnetic and superconducting phases in $Fe_{1+y}Te_{1-x}Se_x$ are summarized in figure 9. Overall, the behavior is consistent with the common belief that static magnetic order competes with superconductivity, while spin fluctuations promote it.

4.1.2. $A_xFe_{2-y}Se_2$ materials. Antiferromagnetic order was found in $TlFe_{2-y}Se_2$ by neutron and Mössbauer measurements [232, 233] long before the recent discovery of

superconductivity in the related $A_xFe_{2-y}Se_2$ compounds. Bao *et al* [188] have recently used neutron powder diffraction to determine the crystalline and magnetic structure for $K_xFe_{2-y}Se_2$. At high temperatures, the crystal structure is equivalent to that of the 122 materials. At lower temperatures, the Fe vacancy order drives the system to an $I4/m$ phase with an enlarged unit cell of $\sqrt{5} \times \sqrt{5} \times 1$ [234], which contains a pair of the Fe–Se layers related by inversion symmetry [188]. It is found that T_N is as high as 559 K and that the magnetic moment is as large as $3.31\mu_B$/Fe, forming a collinear antiferromagnetic structure with (1 0 1) being the propagation wave vector [216]. The moment points mainly along the c-axis [188]. Such a collinear magnetic structure has been reproduced by several theoretical works [199, 200, 218, 235]. It is intriguing that the magnetic order occurs in a tetragonal phase without breaking the four-fold symmetry, although the presence of Fe vacancies may reduce any magnetic frustration [218]. More surprisingly, it has been reported that superconductivity coexists with the strong antiferromagnetic order, both in the neutron study of $K_{0.8}Fe_2Se_2$ [188] and in the muon spin rotation (μSR) study of $Cs_{0.8}Fe_2Se_{1.96}$ [184]. There have been many further observations of the coexistence of superconductivity and antiferromagnetic order [179, 182, 183, 191, 236]. However, due to the difficulty in obtaining samples with high superconducting volume fractions, as well as evidence pointing to phase separations [131, 132, 180, 215, 237–239], it is not yet clear whether the superconductivity and antiferromagnetic order coexist locally or in different regions of a sample.

4.2. Spin excitations in $Fe_{1+y}Te_{1-x}Se_x$

4.2.1. Spin dynamics near (0.5, 0.5). The 'resonance' mode in the magnetic excitations, which is defined as the energy at which there is a significant increase in spectral weight when the system enters the superconducting phase, has been the subject of extensive measurements. The resonance is predicted to occur at a particular wave vector if it connects portions of the Fermi surface that have opposite signs of the superconducting gap function. Therefore, observations of the resonance may provide important information relevant to the pairing symmetry [240–243]. (Note that these analyses make the assumption that the magnetism is due to the same electrons that participate in the superconductivity, while the validity of the assumption is still under debate [114, 223, 229]). Resonance excitations have been observed in a number of iron-based superconductors [77, 82], consistent with the presumed gap-sign change between the hole and electron pockets [209]. In $Fe_{1+y}Te_{1-x}Se_x$, despite the fact that the magnetic ordering wave vector is different from that of iron pnictides by 45°, the resonance excitation was observed to be near the same (0.5, 0.5) wave vector by several groups [83–85, 114, 244–246]. Compared to the magnetic excitation spectrum above T_c, the low-temperature spectral weight is significantly enhanced around (0.5, 0.5) and the resonance energy of ∼6.5 meV, as shown in figure 13(*c*) [83]. The resonance energy corresponds to $\sim 5k_BT_c$, similar to the situation in other high-T_c superconductors [89]. Accompanying the resonance, there is a spin gap with an energy of ∼4 meV; the intensity below the spin gap is shifted to the resonance in the superconducting state [83, 85].

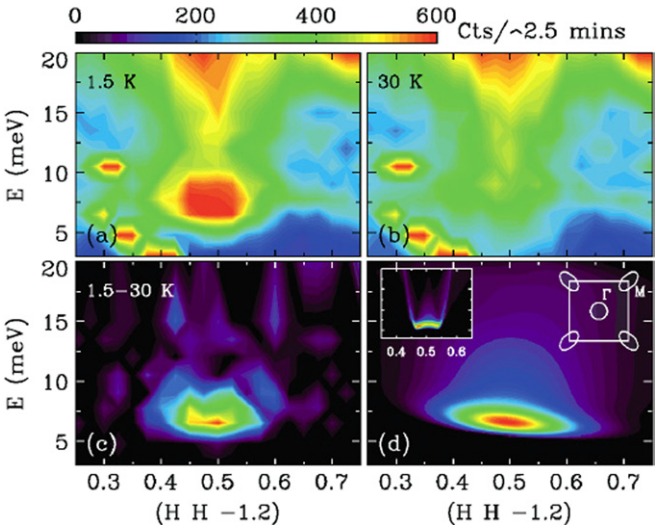


Figure 13. Spin resonance in $FeTe_{0.6}Se_{0.4}$. (*a*) and (*b*) show the spin excitation spectrum as a function of $\boldsymbol{Q}$ and energy at 1.5 K and 30 K, respectively. (*c*) shows the resonance intensity as determined by the difference between the 1.5 and 30 K spectra. (*d*) Calculated intensity difference from a simplified two-band model with resolution convolved. The left inset shows the resolution-free calculated intensity and the right inset is the normal-state Fermi surface employed in the calculation. Reprinted with permission from [83]. Copyright 2009 by the American Physical Society.

Interestingly, it is found that the resonance is incommensurate in $\boldsymbol{Q}$, peaking at $(0.5 \pm \delta, 0.5 \mp \delta)$, in a direction transverse to (0.5, 0.5) [114]. Results on the $\boldsymbol{Q}$ dependence of the magnetic response at 6.5 meV are plotted in figure 14. Transverse scans along $[1\ \bar{1}\ 0]$ exhibit a pair of peaks as shown in figure 14(*a*), while longitudinal scans show a single broad peak centered at (0.5, 0.5), as shown in figure 14(*b*). In both cases, the intensity is enhanced when the sample is cooled below T_c. The color-coded plot of intensity versus $\boldsymbol{Q}$ at 6.5 meV and $T = 1.5$ K, figure 14(*c*), demonstrates an intriguing anisotropy: the transverse peaks are not reproduced along the longitudinal direction.

For other energies, the anisotropy still persists [84, 244–247], showing that the magnetic excitations are anisotropic, dispersing only along the direction transverse to (0.5, 0.5), as shown in figure 14(*d*). This is certainly not a spin-wave-like excitation, as in $CaFe_2As_2$ [248, 249], since in that case one would expect to see a cone-shaped dispersion. ARPES measurements on the sample found that the Fermi surface near (0.5, 0.5) appears to consist of four incommensurate pockets [114]. While Fermi-surface nesting is in principle compatible with the observation of the incommensurate resonance, the dispersion of isolated intensity peaks along a single direction is quite unusual and requires consideration of coupling of spin and orbital effects [114].

Since superconductivity, and hence the pairing, is sensitive to magnetic field, one would naturally expect that an external magnetic field could impact the resonance, as seen in $YBa_2Cu_3O_{6.6}$ [250] and in $La_{1.82}Sr_{0.18}CuO_4$ [251].

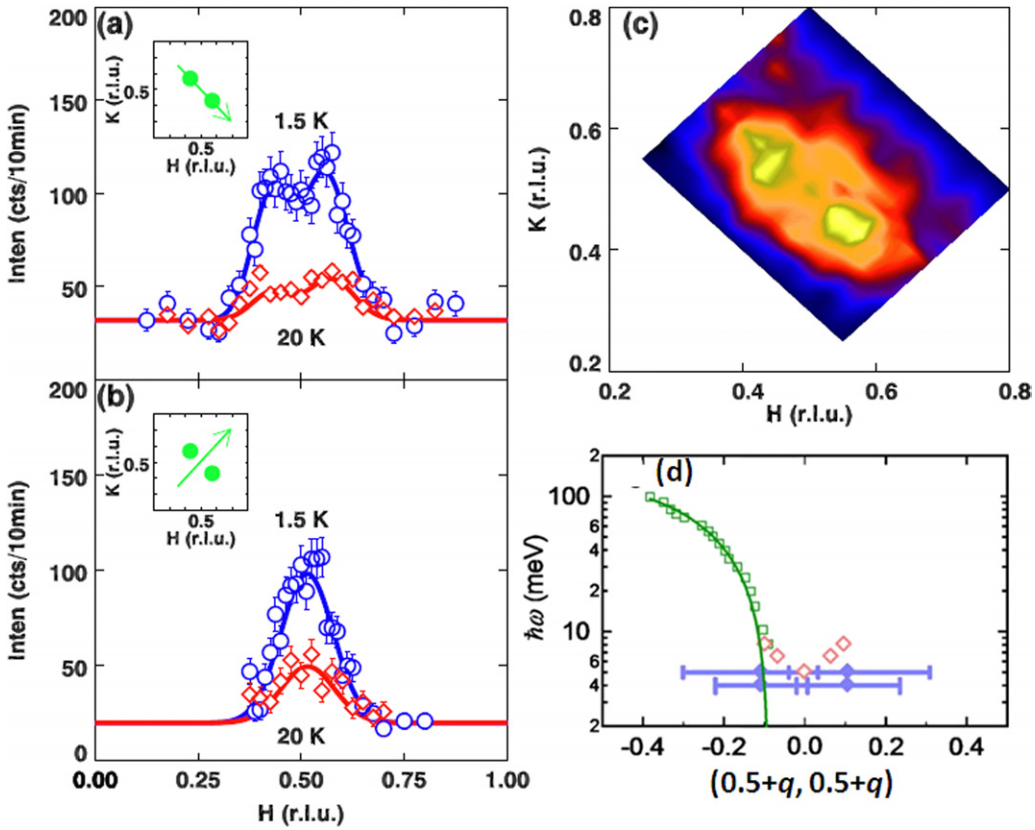


Figure 14. Incommensurate resonance in $\boldsymbol{Q}$, peaking at $(0.5 \pm \delta, 0.5 \mp \delta)$, transversely to $(0.5, 0.5)$, at $\hbar\omega = 6.5$ meV. (*a*) and (*b*) show the $\boldsymbol{Q}$ scans at 1.5 and 20 K, below and above T_c, with scan directions shown in the left insets. Upper right inset is obtained by subtracting 20 K data from 1.5 K data. (*c*) is the plot of the $\boldsymbol{Q}$ dependence of the intensity at 6.5 meV at 1.5 K. (*d*) shows the dispersion from $(0.5, 0.5)$ in semi-log scale. (*a*)–(*c*) reprinted from [126]. (*d*) reprinted with permission from [114]. Copyright 2010 by the American Physical Society.

Qiu *et al* [83] found no significant change in the resonance in $FeTe_{0.6}Se_{0.4}$ in the presence of a 7 T field on a cold-neutron spectrometer with a low flux. Another experiment on $FeTe_{0.5}Se_{0.5}$ using a spectrometer with a higher flux concluded that the resonance starts to appear at a lowered T_c, 12 K, with reduced intensity, due to the suppression of the superconductivity; however, there was no detectable change in either the resonance energy or the width of the resonance peak [85]. With a field of 14.5 T, Zhao *et al* [252] have shown that in $BaFe_{1.9}Ni_{0.1}As_2$, both the resonance energy and intensity are reduced, and the resonance peak is slightly broadened.

One commonly adopted view is that the spin resonance is a singlet-to-triplet excitation [242, 243, 253]. In principle, this hypothesis can be tested by experiments in magnetic field which should induce a Zeeman splitting and lift the degeneracy of the triplet excited state [250]. Bao *et al* [254] tried to address this problem by applying a 14 T field on $FeSe_{0.4}Te_{0.6}$, and it appears that the field induces a peak splitting. However, a more recent experiment shows that the field only reduces the spectral weight around the resonance mode [255]. We applied a 16 T magnetic field and examined the field effect on the resonance. No splitting was observed in this measurement either. The nature of the resonance mode is still an open question.

4.2.2. Doping dependence. As discussed above, the non-superconducting parent compound of the 11 system, $Fe_{1+y}Te$, has static magnetic order with a bicollinear spin configuration. In samples with robust superconducting properties, there is strong magnetic scattering around $(0.5, 0.5)$ with a spin resonance below T_c, corresponding to spin correlations of the collinear type. A number of theoretical [74, 227] and experimental [53, 115, 246, 247] studies have been carried out on the doping evolution of the magnetic correlations (static and dynamic), and their correlation with superconductivity. Lumsden *et al* [247] have performed measurements on time-of-flight spectrometers which cover a large momentum–energy space on two samples, a non-superconducting $Fe_{1.04}Te_{0.73}Se_{0.27}$, and a superconducting $FeTe_{0.51}Se_{0.49}$. It is clearly shown in figure 15(*a*) that at 5–7 meV, for the non-superconducting sample, the spectral weight is mostly concentrated around $(0.5, 0)$, where static magnetic order is observed. For the superconducting sample, magnetic excitations with a spin resonance near $(0.5, 0.5)$ are dominant, as shown in figure 15(*b*). On the other hand, the high-energy (>120 meV) spectrum looks qualitatively similar for these two samples [247]. In the non-superconducting parent compound, $Fe_{1.05}Te$, spin waves dispersing up to ~250 meV have been measured by Lipscombe *et al* [256]. These have been modeled in terms of spin waves calculated from a Heisenberg Hamiltonian with nearest- and next-nearest-neighbor couplings [256]; however, a recent study of $Fe_{1.1}Te$, identifying distinct patterns of diffuse scattering and anomalous thermal enhancement of the effective moment, raises questions about such an approach [229].

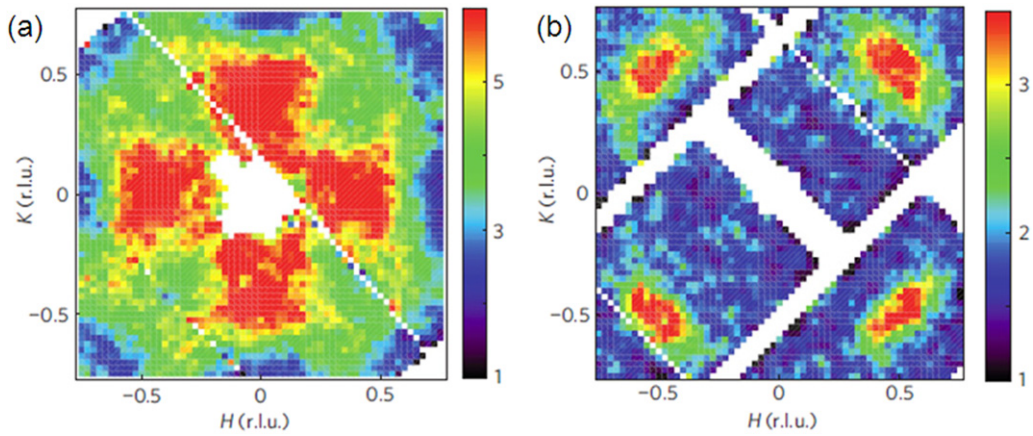


Figure 15. (*a*) Constant-energy cut of the magnetic excitation spectrum at an energy transfer of 6 ± 1 meV for the non-superconducting sample $Fe_{1.04}Te_{0.73}Se_{0.27}$ at 5 K. (*b*) Plot for the superconducting sample $FeTe_{0.51}Se_{0.49}$ at 3.5 K. Reprinted by permission from Macmillan Publishers Ltd: *Nature Phys.* [247], copyright 2010.

As mentioned previously, the properties of $Fe_{1+y}Te_{1-x}Se_x$ are sensitive not only to the Se concentration, but also to the amount of excess Fe. Xu *et al* [115] demonstrated this by measuring the magnetic spectrum around $(0.5, 0)$ and $(0.5, 0.5)$ in four samples: $FeTe_{0.7}Se_{0.3}$, $Fe_{1.05}Te_{0.7}Se_{0.3}$; $FeTe_{0.5}Se_{0.5}$, and $Fe_{1.05}Te_{0.55}Se_{0.45}$. Both samples with $y = 0$ are superconducting with the same T_c of 14 K; a resonance in the spin excitation spectrum is observed below T_c near $(0.5, 0.5)$, although the one with $x = 0.3$ has a smaller superconducting volume fraction, and less spectral weight around $(0.5, 0.5)$. Also, there is short-range static magnetic order near $(0.5, 0)$ in $FeTe_{0.7}Se_{0.3}$, while the sample with $x = 0.5$ does not exhibit magnetic order, short- or long-ranged, and the low-energy excitations close to $(0.5, 0)$ also disappear. With 0.05 extra Fe, superconductivity in both samples is fully suppressed, leading to the absence of the resonance, and the spectral weight transfers from $(0.5, 0.5)$ to $(0.5, 0)$. In both samples, there is short-range static order and strong spectral weight around $(0.5, 0)$. Recently, Stock *et al* [257] have shown that by changing y in $Fe_{1+y}Te$, the low-energy magnetic excitation spectrum can be dramatically modified, thus demonstrating the important role of excess Fe.

4.3. Summary

In the parent compound of the 11 system, there is long-range antiferromagnetic order with an ordering temperature of 65 K, and an in-plane wave vector $(0.5, 0)$; importantly, no Fermi-surface nesting is found along this wave vector. The direction of the wave vector is different from that of the iron pnictides by 45°. The magnetic ordering wave vector can become incommensurate with larger amounts of excess Fe.

Upon Se doping, the antiferromagnetic order is suppressed and becomes short-ranged, followed by the appearance of superconductivity. For samples with $x \approx 0.5$ and robust superconductivity, there is no static order, and the low-energy spin excitations around $(0.5, 0)$ also disappear. The spectral weight is shifted to $(0.5, 0.5)$, where an incommensurate spin resonance is observed; the spin resonance is demonstrated to be intimately tied to the superconductivity from both the temperature and magnetic-field dependence. The magnetic excitation spectrum around $(0.5, 0.5)$ shows an interesting anisotropy, which apparently cannot be explained by either a Fermi-surface-nesting or a local-moment model. In $Fe_{1+y}Se$, there is no static order, while there are spin fluctuations which are enhanced near T_c. The superconducting and magnetic properties of the system can also be modified by adjusting the amount of excess Fe with fixed Se content. The extra Fe is found to enhance the magnetic correlations around $(0.5, 0)$ and suppress superconductivity as well as the spin excitations around $(0.5, 0.5)$.

The results on the evolution of the magnetic excitation spectrum with the tuning parameters (Se/Fe) clearly indicate that static bicollinear magnetic order in the 11 system competes with superconductivity. It appears that only when the system evolves toward fluctuating collinear magnetic correlations, does superconductivity appear; this seems to be universal across all known iron-based superconductor families. Despite these agreements, the origin of the magnetism in the 11 compound is quite controversial. Some believe that the magnetism arises from itinerant electrons [84, 244]. Recently there has been work suggesting a large local moment associated with the low-energy magnetic excitations in a superconducting $FeTe_{0.35}Se_{0.65}$ sample; this observation is incompatible with predictions from a weakly coupled itinerant picture [258]. The fact that a simple Fermi-surface-nesting picture [219] cannot explain many of the experimental observations [114, 137, 220, 258] leads to arguments for a significant local-moment character to the magnetism [42, 220, 223–228].

For the $A_xFe_{2-y}Se_2$ system, it is found that superconductivity is in close proximity to an insulating phase. This feature is different from that in other iron-based superconductors, but mirrors that in the high-T_c cuprates. Whether the microscopic coexistence of strong antiferromagnetic order with high-T_c superconductivity is true or not requires further investigation. If they do coexist, it requires further studies to understand whether or not the superconducting pairing mechanism in this system is the same as that in other high-T_c superconductors.

5. Conclusions

Thanks to the sustained efforts on sample synthesis for the $Fe_{1+y}Te_{1-x}Se_x$ system, some high-quality samples have been made available. In particular, using the Bridgman technique, many large-size, high-quality single crystals have been grown. Measurements performed on these samples yield a plethora of fascinating results. It has been found that the static antiferromagnetic order in the parent compound is centered around the wave vector $(0.5, 0)$ with a bicollinear spin structure that competes with superconductivity, while superconducting samples are characterized by collinear magnetic correlations with magnetic excitations centered around the wave vector $(0.5, 0.5)$. The argument that there is an intimate relationship between the spin excitations around $(0.5, 0.5)$ and superconductivity has been reinforced by the temperature and magnetic-field dependence of the resonance. Generally, this system shows strong similarities to other high-T_c superconductors, where it is believed that spin excitations play a progenitive role in the superconductivity.

For the newly discovered $A_xFe_{2-y}Se_2$ superconductors, which have superconducting transition temperatures, T_c, up to 33 K, crystals can be obtained using the Bridgman technique. This system is unique. (i) It has a very different Fermi-surface topology with two electron pockets at the Brillouin zone center. (ii) The superconducting phase borders an insulating parent phase, as in the case of the cuprates, but different from all previously investigated iron-based superconductors.

While $A_xFe_{2-y}Se_2$ has attracted significant attention, there are still many basic questions to be answered. For instance, reports on the spin dynamics in this system have been very limited [259]. This will provide important clues on whether or not this system shares the same basic physics underlying the superconductivity as other high-temperature superconductors. Also, further efforts on obtaining single crystals with improved sample quality and larger size will certainly be needed in order to elucidate many unresolved issues. For the 11 system, sample inhomogeneity is a less significant issue. Future work to control the stoichiometry more precisely will be helpful.

Acknowledgments

The work at Brookhaven National Laboratory (JW, GX, GG and JMT) was supported by the Office of Basic Energy Sciences, Division of Materials Science and Engineering, U S Department of Energy, under Contract No. DE-AC02-98CH10886. JMT is also supported in part by the Center for Emergent Superconductivity, an Energy Frontier Research Center. Work at Lawrence Berkeley National Laboratory (JW and RJB) was supported by the same Office under Contract No. DE-AC02-05CH11231. The authors thank all of their collaborators listed in the references. The authors are also grateful to their colleagues and collaborators for allowing them to reproduce their work here.

References

[1] Onnes H K The resistance of pure mercury at helium temperatures 1911 *Commun. Leiden.* No 120b

[2] Bardeen J, Cooper L N and Schrieffer J R 1957 Theory of superconductivity *Phys. Rev.* **108** 1175

[3] Bednorz J G and Müller K A 1986 Possible high T_c superconductivity in the Ba–La–Cu–O system *Z. Phys.* B **64** 189

[4] Wu M K, Ashburn J R, Torng C J, Hor P H, Meng R L, Gao L, Huang Z J, Wang Y Q and Chu C W 1987 Superconductivity at 93 K in a new mixed-phase Y–Ba–Cu–O compound system at ambient pressure *Phys. Rev. Lett.* **58** 908

[5] Lee P A, Nagaosa N and Wen X G 2006 Doping a Mott insulator: physics of high-temperature superconductivity *Rev. Mod. Phys.* **78** 17

[6] Carlson E W, Emery V J, Kivelson S A and Orgad D 2002 Concepts in high temperature superconductivity *The Physics of Conventional and Unconventional Superconductors* (Berlin: Springer)

[7] Birgeneau R J, Stock C, Tranquada J M and Yamada K 2006 Magnetic neutron scattering in hole doped cuprate superconductors *J. Phys. Soc. Japan* **75** 111003

[8] Kastner M A, Birgeneau R J, Shirane G and Endoh Y 1998 Magnetic, transport, and optical properties of monolayer copper oxides *Rev. Mod. Phys.* **70** 897

[9] Orenstein J and Millis A J 2000 Advances in the physics of high-temperature superconductivity *Science* **288** 468

[10] Kamihara Y, Hiramatsu H, Hirano M, Kawamura R, Yanagi H, Kamiya T and Hosono H 2006 Iron-based layered superconductor: LaOFeP *J. Am. Chem. Soc.* **128** 10012

[11] Kamihara Y, Watanabe T, Hirano M and Hosono H 2008 Iron-based layered superconductor $La[O_{1-x}F_x]FeAs$ ($x = 0.05$–0.12) with $T_c = 26$ K *J. Am. Chem. Soc.* **130** 3296

[12] Chen X H, Wu T, Wu G, Liu R H, Chen H and Fang D F 2008 Superconductivity at 43 K in samarium-arsenide oxides $SmFeAsO_{1-x}F_x$ *Nature* **453** 761

[13] Takahashi H, Igawa K, Arii K, Kamihara Y, Hirano M and Hosono H 2008 Superconductivity at 43 K in an iron-based layered compound $LaO_{1-x}F_xFeAs$ *Nature* **453** 376

[14] Kito H, Eisaki H and Iyo A 2008 Superconductivity at 54 K in F-free $NdFeAsO_{1-y}$ *J. Phys. Soc. Japan* **77** 063707

[15] Ren Z-A *et al* 2008 Superconductivity in the iron-based F-doped layered quaternary compound $NdO_{1-x}F_xFeAs$ *Europhys. Lett.* **82** 57002

[16] Ren Z-A *et al* 2008 Superconductivity at 55 K in iron-based F-doped layered quaternary compound $SmO_{1-x}F_xFeAs$ *Chin. Phys. Lett.* **25** 2215

[17] Wang C *et al* 2008 Thorium-doping-induced superconductivity up to 56 K in $Gd_{1-x}Th_xFeAsO$ *Europhys. Lett.* **83** 67006

[18] Sefat A S, Jin R, McGuire M A, Sales B C, Singh D J and Mandrus D 2008 Superconductivity at 22 K in Co-doped $BaFe_2As_2$ crystals *Phys. Rev. Lett.* **101** 117004

[19] Rotter M, Tegel M and Johrendt D 2008 Superconductivity at 38 K in the iron arsenide $Ba_{1-x}K_xFe_2As_2$ 2008 *Phys. Rev. Lett.* **101** 107006

[20] Chen G F, Li Z, Li G, Hu W Z, Dong J, Zhang X D, Zheng P, Wang N L and Luo J L 2008 Superconductivity in hole-doped $(Sr_{1-x}K_x)Fe_2As_2$ *Chin. Phys. Lett.* **25** 3403

[21] Inosov D S *et al* 2009 Suppression of the structural phase transition and lattice softening in slightly underdoped $Ba_{1-x}K_xFe_2As_2$ with electronic phase separation *Phys. Rev.* B **79** 224503

[22] Deng Z, Wang X C, Liu Q Q, Zhang S J, Lv Y X, Zhu J L, Yu R C and Jin C Q 2009 A new "1 1 1" type iron pnictide superconductor LiFeP *Europhys. Lett.* **87** 37004

[23] Wang X C, Liu Q Q, Lv Y X, Gao W B, Yang L X, Yu R C, Li F Y and Jin C Q. 2008 The superconductivity at 18 K in LiFeAs system *Solid State Commun.* **148** 538

[24] Pitcher M J, Parker D R, Adamson P, Herkelrath S J C, Boothroyd A T and Clarke S J 2008 Structure and superconductivity of LiFeAs *Chem. Commun.* **45** 5918

[25] Chu C W, Chen F, Gooch M, Guloy A M, Lorenz B, Lv B, Sasmal K, Tang Z J, Tapp J H and Xue Y Y 2009 The synthesis and characterization of LiFeAs and NaFeAs *Physica* C **469** 326

[26] Tapp J H, Tang Z, Lv B, Sasmal K, Lorenz B, Chu P C W and Guloy A M 2008 LiFeAs: an intrinsic FeAs-based superconductor with $T_c = 18$ K *Phys. Rev.* B **78** 060505

[27] Zhang S J *et al* 2009 Superconductivity at 31 K in the '1 1 1 '-type iron arsenide superconductor $Na_{1-x}FeAs$ induced by pressure *Europhys. Lett.* **88** 47008

[28] Hsu F-C *et al* 2008 Superconductivity in the PbO-type structure α-FeSe *Proc. Natl Acad. Sci. USA* **105** 14262

[29] Yeh K-W *et al* 2008 Tellurium substitution effect on superconductivity of the α-phase iron selenide *Europhys. Lett.* **84** 37002

[30] Sales B C, Sefat A S, McGuire M A, Jin R Y, Mandrus D and Mozharivskyj Y 2009 Bulk superconductivity at 14 K in single crystals of $Fe_{1+y}Te_xSe_{1-x}$ *Phys. Rev.* B **79** 094521

[31] Chen G F, Chen Z G, Dong J, Hu W Z, Li G, Zhang X D, Zheng P, Luo J L and Wang N L 2009 Electronic properties of single-crystalline $Fe_{1.05}Te$ and $Fe_{1.03}Se_{0.30}Te_{0.70}$ *Phys. Rev.* B **79** 140509(R)

[32] Fang M H, Pham H M, Qian B, Liu T J, Vehstedt E K, Liu Y, Spinu L and Mao Z Q 2008 Superconductivity close to magnetic instability in $Fe(Se_{1-x}Te_x)_{0.82}$ *Phys. Rev.* B **78** 224503

[33] Zhu X, Han F, Mu G, Cheng P, Shen B, Zeng B and Wen H-H 2009 Transition of stoichiometric Sr_2VO_3FeAs to a superconducting state at 37.2 K *Phys. Rev.* B **79** 220512

[34] Ogino H, Matsumura Y, Katsura Y, Ushiyama K, Horii S, Kishio K and Shimoyama J I 2009 Superconductivity at 17 K in $(Fe_2P_2)(Sr_4Sc_2O_6)$: a new superconducting layered pnictide oxide with a thick perovskite oxide layer *Supercond. Sci. Technol.* **22** 075008

[35] Zhao J *et al* 2008 Lattice and magnetic structures of PrFeAsO, $PrFeAsO_{0.85}F_{0.15}$ and $PrFeAsO_{0.85}$ *Phys. Rev.* B **78** 132504

[36] Lester C, Chu J-H, Analytis J G, Capelli S C, Erickson A S, Condron C L, Toney M F, Fisher I R and Hayden S M 2009 Neutron scattering study of the interplay between structure and magnetism in $Ba(Fe_{1-x}Co_x)_2As_2$ *Phys. Rev.* B **79** 144523

[37] Qiu Y *et al* 2008 Crystal structure and antiferromagnetic order in $NdFeAsO_{1-x}F_x$ ($x = 0.0$ and 0.2) superconducting compounds from neutron diffraction measurements *Phys. Rev. Lett.* **101** 257002

[38] Kumar N, Chi S, Chen Y, Rana K G, Nigam A K, Thamizhavel A, Ratcliff W II, Dhar S K and Lynn J W 2009 Evolution of the bulk properties, structure, magnetic order, and superconductivity with Ni doping in $CaFe_{2-x}Ni_xAs_2$ *Phys. Rev.* B **80** 144524

[39] de la Cruz C *et al* 2008 Magnetic order close to superconductivity in the iron-based layered $LaO_{1-x}F_xFeAs$ systems *Nature* **453** 899

[40] Huang Q, Qiu Y, Bao W, Green M A, Lynn J W, Gasparovic Y C, Wu T, Wu G and Chen X H 2008 Neutron-diffraction measurements of magnetic order and a structural transition in the parent $BaFe_2As_2$ compound of FeAs-based high-temperature superconductors *Phys. Rev. Lett.* **101** 257003

[41] Chen Y, Lynn J W, Li J, Li G, Chen G F, Luo J L, Wang N L, Dai P, de la Cruz C and Mook H A 2008 Magnetic order of the iron spins in NdFeAsO *Phys. Rev.* B **78** 064515

[42] Johannes M D and Mazin I I 2009 Microscopic origin of magnetism and magnetic interactions in ferropnictides *Phys. Rev.* B **79** 220510(R)

[43] Wilson S D, Yamani Z, Rotundu C R, Freelon B, Bourret-Courchesne E and Birgeneau R J 2009 Neutron diffraction study of the magnetic and structural phase transitions in $BaFe_2As_2$ *Phys. Rev.* B **79** 184519

[44] Kofu M, Qiu Y, bao W, Lee S H, Chang S, Wu T, Wu G and Chen X H 2009 Neutron scattering investigation of the magnetic order in single crystalline $BaFe_2As_2$ *New J. Phys.* **11** 055001

[45] Zhao J *et al* 2008 Structural and magnetic phase diagram of $CeFeAsO_{1-x}F_x$ and its relation to high-temperature superconductivity *Nature Mater.* **7** 953

[46] Luetkens H *et al* 2009 The electronic phase diagram of the $LaO_{1-x}F_xFeAs$ superconductor *Nature Mater.* **8** 305

[47] Drew A J *et al* 2009 Coexistence of static magnetism and superconductivity in $SmFeAsO_{1-x}F_x$ as revealed by muon spin rotation *Nature Mater.* **8** 310

[48] Rotter M, Pangerl M, Tegel M and Johrendt D 2008 Superconductivity and crystal structures of $(Ba_{1-x}K_x)Fe_2As_2$ ($x = 0$–1) *Angew. Chem. Int. Edn Engl.* **47** 7949

[49] Chen H *et al* 2009 Coexistence of the spin-density-wave and superconductivity in the $(Ba,K)Fe_2As_2$ *Europhys. Lett.* **85** 17006

[50] Fang L *et al* 2009 Roles of multiband effects and electron-hole asymmetry in the superconductivity and normal-state properties of $Ba(Fe_{1-x}Co_x)_2As_2$ *Phys. Rev.* B **80** 140508(R)

[51] Chu J-H, Analytis J G, Kucharczyk C and Fisher I R 2009 Determination of the phase diagram of the electron-doped superconductor $Ba(Fe_{1-x}Co_x)_2As_2$ *Phys. Rev.* B **79** 014506

[52] Khasanov R *et al* 2009 Coexistence of incommensurate magnetism and superconductivity in $Fe_{1+y}Se_xTe_{1-x}$ *Phys. Rev.* B **80** 140511

[53] Liu T J *et al* 2010 From $(\pi, 0)$ magnetic order to superconductivity with (π, π) magnetic resonance in $Fe_{1.02}(Te_{1-x}Se_x)$ *Nature Mater.* **9** 716

[54] Paulose P L, Yadav C S and Subhedar K M 2010 Magnetic phase diagram of $Fe_{1.1}Te_{1-x}Se_x$: a comparative study with the stoichiometric superconducting $FeTe_{1-x}Se_x$ system *Europhys. Lett.* **90** 27011

[55] Katayama K *et al* 2010 Investigation of the spin-glass regime between the antiferromagnetic and superconducting phases in $Fe_{1+y}Se_xTe_{1-x}$ *J. Phys. Soc. Japan* **79** 113702

[56] Mizuguchi Y and Takano Y 2010 Review of Fe chalcogenides as the simplest Fe-based superconductor *J. Phys. Soc. Japan* **79** 102001

[57] Dong C, Wang H, Li Z, Chen J, Yuan H Q and Fang M 2010 Revised phase diagram for $FeTe_{1-x}Se_x$ system with less excess Fe atoms arXiv:1012.5188

[58] Huang Q, Zhao J, Lynn J W, Chen G F, Luo J L, Wang N L and Dai P 2008 Doping evolution of antiferromagnetic order and structural distortion in $LaFeAsO_{1-x}F_x$ *Phys. Rev.* B **78** 054529

[59] Michael A *et al* 2008 Phase transitions in LaFeAsO: structural, magnetic, elastic, and transport properties, heat capacity and Mössbauer spectra *Phys. Rev.* B **78** 094517

[60] Kivelson S A and Yao H 2008 Iron-based superconductors: unity or diversity? *Nature Mater.* **7** 927

[61] Mazin I I, Singh D J, Johannes M D and Du M H 2008 Unconventional superconductivity with a sign reversal in

the order parameter of $LaFeAsO_{1-x}F_x$ *Phys. Rev. Lett.* **101** 057003
[62] Kuroki K, Onari S, Arita R, Usui H, Tanaka Y, Kontani H and Aoki H 2008 Unconventional pairing originating from the disconnected Fermi surfaces of superconducting $LaFeAsO_{1-x}F_x$ *Phys. Rev. Lett.* **101** 087004
[63] Ma F and Lu Z-Y 2008 Iron-based layered compound LaFeAsO is an antiferromagnetic semimetal *Phys. Rev.* B **78** 033111
[64] Dong J *et al* 2008 Competing orders and spin-density-wave instability in $La(O_{1-x}F_x)FeAs$ *Europhys. Lett.* **83** 27006
[65] Cvetkovic V and Tesanovic Z 2009 Multiband magnetism and superconductivity in Fe-based compounds *Europhys. Lett.* **85** 37002
[66] Graser S, Maier T A, Hirschfeld P J and Scalapino D J 2009 Near-degeneracy of several pairing channels in multiorbital models for the Fe pnictides *New J. Phys.* **11** 025016
[67] Kotegawa H, Masaki S, Awai Y, Tou H, Mizuguchi Y and Takano Y 2008 Evidence for unconventional superconductivity in arsenic-free iron-based superconductor FeSe: a ^{77}Se-NMR study *J. Phys. Soc. Japan* **77** 113703
[68] Fang C, Yao H, Tsai W F, Hu J P and Kivelson S A 2008 Theory of electron nematic order in LaOFeAs *Phys. Rev.* B **77** 224509
[69] Haule K and Kotliar G 2009 Coherence–incoherence crossover in the normal state of iron oxypnictides and importance of Hund's rule coupling *New J. Phys.* **11** 025021
[70] Si Q, Abrahams E, Dai J and Zhu J-X 2009 Correlation effects in the iron pnictides *New J. Phys.* **11** 045001
[71] Mazin I I and Johannes M D 2009 A key role for unusual spin dynamics in ferropnictides *Nature Phys.* **5** 141
[72] Kou S-P, Li T and Weng Z-y 2009 Coexistence of itinerant electrons and local moments in iron-based superconductors *Euro. Phys. Lett.* **88** 17010
[73] de' Medici L, Hassan S R and Capone M 2009 Genesis of coexisting itinerant and localized electrons in iron pnictides *J. Supercond. Nov. Magn.* **22** 535
[74] Yin W-G, Lee C-C and Ku W 2010 Unified picture for magnetic correlations in iron-based superconductors *Phys. Rev. Lett.* **105** 107004
[75] Arita R and Ikeda H 2009 Is Fermi-surface nesting the origin of superconductivity in iron pnictides?: a fluctuation–exchange-approximation study *J. Phys. Soc. Japan* **78** 113707
[76] Kontani H and Onari S 2010 Orbital-fluctuation-mediated superconductivity in iron pnictides: analysis of the five-orbital Hubbard–Holstein model *Phys. Rev. Lett.* **104** 157001
[77] Christianson A D *et al* 2008 Unconventional superconductivity in $Ba_{0.6}K_{0.}4Fe_2As_2$ from inelastic neutron scattering *Nature* **456** 930
[78] Lumsden M D *et al* 2009 Two-dimensional resonant magnetic excitation in $BaFe_{1.84}Co_{0.16}As_2$ *Phys. Rev. Lett.* **102** 107005
[79] Chi S *et al* 2009 Inelastic neutron-scattering measurements of a three-dimensional spin resonance in the FeAs-based $BaFe_{1.9}Ni_{0.1}As_2$ superconductor *Phys. Rev. Lett.* **102** 107006
[80] Li S, Chen Y, Chang S, Lynn J W, Li L, Luo Y, Cao G, Xu Z and Dai P 2009 Spin gap and magnetic resonance in superconducting $BaFe_{1.9}Ni_{0.1}As_2$ *Phys. Rev.* B **79** 174527
[81] Inosov D S *et al* 2010 Normal-state spin dynamics and temperature-dependent spin resonance energy in an optimally doped iron arsenide superconductor *Nature Phys.* **6** 178
[82] Shamoto S-i, Ishikado M, Christianson A D, Lumsden M D, Wakimoto S, Kodama K, Iyo A and Arai M 2010 Inelastic neutron scattering study of the resonance mode in the optimally doped pnictide superconductor $LaFeAsO_{0.92}F_{0.08}$ *Phys. Rev.* B **82** 172508
[83] Qiu Y *et al* 2009 Spin gap and resonance at the nesting wave vector in superconducting $FeSe_{0.4}Te_{0.6}$ *Phys. Rev. Lett.* **103** 067008
[84] Mook H A *et al* 2010 Unusual relationship between magnetism and superconductivity in $FeTe_{0.5}Se_{0.5}$ *Phys. Rev. Lett.* **104** 187002
[85] Wen J, Xu G, Xu Z, Lin Z W, Li Q, Chen Y, Chi S, Gu G and Tranquada J M 2010 Effect of magnetic field on the spin resonance in $FeTe_{0.5}Se_{0.5}$ as seen via inelastic neutron scattering *Phys. Rev.* B **81** 100513(R)
[86] Ishida K, Nakai Y and Hosono H 2009 To what extent iron-pnictide new superconductors have been clarified: a progress report *J. Phys. Soc. Japan* **78** 062001
[87] Hosono H 2008 Layered iron pnictide superconductors: discovery and current status *J. Phys. Soc. Japan Suppl.* C **77** 1
[88] Lynn J W and Dai P 2009 Neutron studies of the iron-based family of high T_C magnetic superconductors *Physica* C **469** 469
[89] Lumsden M D and Christianson A D 2010 Magnetism in Fe-based superconductors *J. Phys.: Condens. Matter* **22** 203203
[90] Hosono H 2009 Two classes of superconductors discovered in our material research: iron-based high temperature superconductor and electride superconductor *Physica* C **469** 314
[91] Wu M K *et al* 2009 The development of the superconducting PbO-type β-FeSe and related compounds *Physica* C **469** 340
[92] Canfield P C and Bud'ko S L 2010 FeAs-based superconductivity: a case study of the effects of transition metal doping on $BaFe_2As_2$ *Annu. Rev. Condens. Matter Phys.* **1** 27
[93] Johnston D C 2010 The puzzle of high temperature superconductivity in layered iron pnictides and chalcogenides *Adv. Phys.* **59** 803
[94] Mazin I 2010 Superconductivity gets an iron boost *Nature* **464** 183
[95] Paglione J and Greene R L 2010 High-temperature superconductivity in iron-based materials *Nature Phys.* **6** 645
[96] Guo J, Jin S, Wang G, Wang S, Zhu K, Zhou T, He M and Chen X 2010 Superconductivity in the iron selenide $K_xFe_2Se_2$ ($0 \leqslant x \leqslant 1.0$) *Phys. Rev.* B **82** 180520
[97] Mizuguchi Y, Takeya H, Kawasaki Y, Ozaki T, Tsuda S, Yamaguchi T and Takano Y 2011 Transport properties of the new Fe-based superconductor $K_xFe_2Se_2$ ($T_c = 33$ K) *Appl. Phys. Lett.* **98** 042511
[98] Wang A F *et al* 2011 Superconductivity at 32 K in single-crystalline $Rb_xFe_{2-y}Se_2$ *Phys. Rev.* B **83** 060512
[99] Krzton-Maziopa S, Shermadini Z, Pomjakushina E, Pomjakushin V, Bendele M, Amato A, Khasanov R, Luetkens H and Conder K 2011 Synthesis and crystal growth of $Cs_{0.8}(FeSe_{0.98})_2$: a new iron-based superconductor with $T_c = 27$ K *J. Phys.: Condens. Matter* **23** 052203
[100] Wang H-D, Dong C-H, Li Z-J, Mao Q-H, Zhu S-S, Feng C-M, Yuan H Q and Fang M-H 2011 Superconductivity at 32 K and anisotropy in $Tl_{0.58}Rb_{0.42}Fe_{1.72}Se_2$ crystals *Europhys. Lett.* **93** 47004
[101] Okamoto H 1991 The Fe–Se (iron-selenium) system *J. Phase Equilib.* **12** 383

[102] McQueen T M *et al* 2009 Extreme sensitivity of superconductivity to stoichiometry in $Fe_{1+\delta}Se$ *Phys. Rev.* B **79** 014522

[103] Patel U, Hua J, Yu S H, Avci S, Xiao Z L, Claus H, Schlueter J, Vlasko-Vlasov V V, Welp U and Kwok W K 2009 Growth and superconductivity of $FeSe_x$ crystals *Appl. Phys. Lett.* **94** 082508

[104] Zhang S B *et al* 2009 Crystal growth and superconductivity of $FeSe_x$ *Supercond. Sci. Technol.* **22** 015020

[105] Hu R, Lei H, Abeykoon M, Bozin E S, Billinge S J L, Warren J B, Siegrist T and Petrovic C 2011 Synthesis, crystal structure, and magnetism of β-$Fe_{1.00(2)}Se_{1.00(3)}$ single crystals *Phys. Rev.* B **83** 224502

[106] Mok B H *et al* 2009 Growth and investigation of crystals of the new superconductor α-FeSe from KCl solutions *Cryst. Growth Des.* **9** 3260

[107] Okamoto H and Tanner L E 1990 Fe–Te (iron-tellurium) *Binary Alloy Phase Diagrams* **2** 1781

[108] Mizuguchi Y, Deguchi K, Kawasaki Y, Ozaki T, Nagao M, Tsuda S, Yamaguchi T and Takano Y 2011 Superconductivity in oxygen-annealed $FeTe_{1-x}S_x$ single crystal *J. Appl. Phys.* **109** 013914

[109] Liu T J *et al* 2009 Charge-carrier localization induced by excess Fe in the superconductor $Fe_{1+y}Te_{1-x}Se_x$ *Phys. Rev.* B **80** 174509

[110] Noji T, Suzuki T, Abe H, Adachi T, Kato M and Koike Y 2010 Growth, annealing effects on superconducting and magnetic properties, and anisotropy of $FeSe_{1-x}Te_x$ ($0.5 \leqslant x \leqslant 1$) single crystals *J. Phys. Soc. Japan* **79** 084711

[111] Yang J, Matsui M, Kawa M, Ohta H, Michioka C, Dong C, Wang H, Yuan H , Fang M and Yoshimura K 2010 Magnetic and superconducting properties in single crystalline $Fe_{1+\delta}Te_{1-x}Se_x$ ($x < 0.50$) system *J. Phys. Soc. Japan* **79** 074704

[112] Wen J, Xu G, Xu Z, Lin Z W, Li Q, Ratcliff W, Gu G and Tranquada J M 2009 Short-range incommensurate magnetic order near the superconducting phase boundary in $Fe_{1+\delta}Te_{1-x}Se_x$ *Phys. Rev.* B **80** 104506

[113] Homes C C, Akrap A, Wen J S, Xu Z J, Lin Z W, Li Q and Gu G D 2010 Electronic correlations and unusual superconducting response in the optical properties of the iron-chalcogenide $FeTe_{0.55}Se_{0.45}$ *Phys. Rev.* B **81** 180508(R)

[114] Lee S-H *et al* 2010 Coupling of spin and orbital excitations in the iron-based superconductor $FeTe_{0.5}Se_{0.5}$ *Phys. Rev.* B **81** 220502(R)

[115] Xu Z, Wen J, Xu G, Jie Q, Lin Z, Li Q, Chi S, Singh D K, Gu G and Tranquada J M 2010 Disappearance of static magnetic order and evolution of spin fluctuations in $Fe_{1+\delta}Se_xTe_{1-x}$ *Phys. Rev.* B **82** 104525

[116] Pallecchi I, Lamura G, Tropeano M, Putti M, Viennois R, Giannini E and D. Van der Marel 2009 Seebeck effect in $Fe_{1+x}Te_{1-y}Se_y$ single crystals *Phys. Rev.* B **80** 214511

[117] Taen T, Tsuchiya Y, Nakajima Y and Tamegai T 2009 Superconductivity at $T_c \sim 14$ K in single-crystalline $FeTe_{0.61}Se_{0.39}$ *Phys. Rev.* B **80** 092502

[118] Fang M, Yang J, Balakirev F F, Kohama Y, Singleton J, Qian B, Mao Z Q, Wang H and Yuan H Q 2010 Weak anisotropy of the superconducting upper critical field in $Fe_{1.11}Te_{0.6}Se_{0.4}$ single crystals *Phys. Rev.* B **81** 020509

[119] Hu R, Bozin E S, Warren J B and Petrovic C 2009 Superconductivity, magnetism, and stoichiometry of single crystals of $Fe_{1+y}(Te_{1-x}S_x)_z$ *Phys. Rev.* B **80** 214514

[120] Yeh K W, Ke C T, Huang T W, Chen T K, Huang Y L, Wu P M and Wu M K 2009 Superconducting $FeSe_{1-x}Te_x$ single crystals grown by optical zone-melting technique *Cryst. Growth Des.* **9** 4847

[121] Wang D M, He J B, Xia T-L and Chen G F 2011 Effect of varying iron content on the transport properties of the potassium-intercalated iron selenide $K_xFe_{2-y}Se_2$ *Phys. Rev.* B **83** 132502

[122] Lei H and Petrovic C 2011 Anisotropy in transport and magnetic properties of $K_{0.64}Fe_{1.44}Se_2$ *Phys. Rev.* B **83** 184504

[123] Ying J J *et al* 2011 Superconductivity and magnetic properties of single crystals of $K_{0.75}Fe_{1.66}Se_2$ and $Cs_{0.81}Fe_{1.61}Se_2$ *Phys. Rev.* B **83** 212502

[124] Fang M-H, Wang H-D, Dong C-H, Li Z-J, Feng C-M, Chen J and Yuan H Q 2011 Fe-based superconductivity with $T_c = 31$ K bordering an antiferromagnetic insulator in $(Tl,K)Fe_xSe_2$ *Europhys. Lett.* **94** 27009

[125] Gao Z, Qi Y, Wang L, Yao C, Wang D, Zhang X and Ma Y 2011 Upper fields and critical current density of $K_{0.58}Fe_{1.56}Se_2$ single crystals grown by one step technique arXiv:1103.2904

[126] Wen J 2010 Interplay between magnetism and superconductivity in high-temperature superconductors $La_{2-x}Ba_xCuO_4$ and $Fe_{1+y}Te_{1-x}Se_x$: crystal growth and neutron scattering studies *PhD Thesis* Stony Brook University

[127] Xu Z, Wen J, Xu G, Han S, Li Q, Tranquada J M and Gu G 2011 unpublished

[128] Joseph B, Iadecola A, Puri A, Simonelli L, Mizuguchi Y, Takano Y and Saini N L 2010 Evidence of local structural inhomogeneity in $FeSe_{1-x}Te_x$ from extended x-ray absorption fine structure *Phys. Rev.* B **82** 020502(R)

[129] Hu H, Zuo J M, Wen J S, Xu Z J, Lin Z W, Li Q, Gu G, Park W K and Greene L H 2011 Phase separation and chemical inhomogeneity in the iron chalcogenide superconductor $Fe_{1+y}Te_xSe_{1-x}$ *New J. Phys.* **13** 053031

[130] He X, Li G, Zhang J, Karki A B, Jin R, Sales B C, Sefat A S, McGuire M A, Mandrus D and Plummer E W 2011 Nanoscale chemical phase separation in $FeTe_{0.55}Se_{0.45}$ as seen via scanning tunneling spectroscopy *Phys. Rev.* B **83** 220502

[131] Wang Z, Song Y J, Shi H L, Wang Z W, Chen Z, Tian H F, Chen G F, Guo J G, Yang H X and Li J Q 2011 Microstructure and ordering of iron vacancies in the superconductor system $K_yFe_xSe_2$ as seen via transmission electron microscopy *Phys. Rev.* B **83** 140505

[132] Chen F *et al* 2011 Electronic identification of the actual parental phase of $K_xFe_{2-y}Se_2$ superconductor and its intrinsic mesoscopic phase separation arXiv:1106.3026

[133] Margadonna S, Takabayashi Y, McDonald M T, Kasperkiewicz K, Mizuguchi Y, Takano Y, Fitch A N, Suard E and Prassides K 2008 Crystal structure of the new $FeSe_{1-x}$ superconductor *Chem. Commun.* 5607

[134] Pomjakushina E, Conder K, Pomjakushin V, Bendele M and Khasanov R 2009 Synthesis, crystal structure, and chemical stability of the superconductor $FeSe_{1-x}$ *Phys. Rev.* B **80** 024517

[135] Liu X, Lee C C, Xu Z J, Wen J S, Gu G, Ku W, Tranquada J M and Hill J P 2011 X-ray diffuse scattering study of local distortions in $Fe_{1+x}Te$ induced by excess Fe *Phys. Rev.* B **83** 184523

[136] McQueen T M, Williams A J, Stephens P W, Tao J, Zhu Y, Ksenofontov V, Casper F, Felser C and Cava R J 2009 Tetragonal-to-orthorhombic structural phase transition at 90 K in the superconductor $Fe_{1.01}Se$ *Phys. Rev. Lett.* **103** 057002

[137] Bao W *et al* 2009 Tunable $(\delta\pi, \delta\pi)$-type antiferromagnetic order in α-Fe(Te,Se) superconductors *Phys. Rev. Lett.* **102** 247001

[138] Li S *et al* 2009 First-order magnetic and structural phase transitions in $Fe_{1+y}Se_xTe_{1-x}$ *Phys. Rev.* B **79** 054503

[139] Martinelli A, Palenzona A, Tropeano M, Ferdeghini C, Putti M, Cimberle M R, Nguyen T D, Affronte M and Ritter C 2010 From antiferromagnetism to superconductivity in $Fe_{1+y}Te_{1-x}Se_x$ ($0 \leqslant x \leqslant 0.20$): neutron powder diffraction analysis *Phys. Rev.* B **81** 094115

[140] Mizuguchi Y, Tomioka F, Tsuda S, Yamaguchi T and Takano Y 2009 Superconductivity in S-substituted FeTe *Appl. Phys. Lett.* **94** 012503

[141] Mizuguchi Y, Tomioka F, Tsuda S, Yamaguchi T and Takano Y 2009 FeTe as a candidate material for new iron-based superconductor *Physica* C **469** 1027

[142] Mizuguchi Y, Tomioka F, Tsuda S, Yamaguchi T and Takano Y 2009 Substitution effects on FeSe superconductor *J. Phys. Soc. Japan* **78** 074712

[143] Si W, Lin Z-W, Jie Q, Yin W-G, Zhou J, Gu G, Johnson P D and Li Q 2009 Enhanced superconducting transition temperature in $FeSe_{0.5}Te_{0.5}$ thin films *Appl. Phys. Lett.* **95** 052504

[144] Tsukada I *et al* 2011 Epitaxial growth of $FeSe_{0.5}Te_{0.5}$ thin films on CaF_2 substrates with high critical current density *Appl. Phys. Express* **4** 053101

[145] Imai Y, Tanaka R, Akiike T, Hanawa M, Tsukada I and Maeda A 2010 Superconductivity of $FeSe_{0.5}Te_{0.5}$ thin films grown by pulsed laser deposition *Japan J. Appl. Phys.* **49** 023101

[146] Wu M K *et al* 2010 The development of the superconducting tetragonal PbO-type FeSe and related compounds *Phys. Status Solidi* b **247** 500

[147] Kida T, Matsunaga T, Hagiwara M, Mizuguchi Y, Takano Y and Kindo K 2009 Upper critical fields of the 11-system iron-chalcogenide superconductor $FeSe_{0.25}Te_{0.75}$ *J. Phys. Soc. Japan* **78** 113701

[148] Yadav C S and Paulose P L 2009 Upper critical field, lower critical field and critical current density of $FeTe_{0.60}$ $Se_{0.40}$ single crystals *New J. Phys.* **11** 103046

[149] Rößler S, Cherian D, Harikrishnan S, Bhat H L, Elizabeth S, Mydosh J A, Tjeng L H, Steglich F and Wirth S 2010 Disorder-driven electronic localization and phase separation in superconducting $Fe_{1+y}Te_{0.5}Se_{0.5}$ single crystals *Phys. Rev.* B **82** 144523

[150] Bendele M, Babkevich P, Katrych S, Gvasaliya S N, Pomjakushina E, Conder K, Roessli B, Boothroyd A T, Khasanov R and Keller H 2010 Tuning the superconducting and magnetic properties of $Fe_ySe_{0.25}Te_{0.75}$ by varying the iron content *Phys. Rev.* B **82** 212504

[151] Rodriguez E E, Stock C, Hsieh P, Butch N, Paglione J and Green M A 2011 Chemical control of interstitial iron leading to superconductivity in $Fe_{1+x}Te_{0.7}Se_{0.3}$ *Chem. Sci.* **2** 1782

[152] Medvedev S *et al* 2009 Electronic and magnetic phase diagram of α-$Fe_{1.01}Se$ with superconductivity at 36.7 K under pressure *Nature Mater.* **8** 630

[153] Margadonna S, Takabayashi Y, Ohishi Y, Mizuguchi Y, Takano Y, Kagayama T, Nakagawa T, Takata M and Prassides K 2009 Pressure evolution of the low-temperature crystal structure and bonding of the superconductor FeSe (T_c = 37 K) *Phys. Rev.* B **80** 064506

[154] Masaki S, Kotegawa H, Hara Y, Tou H, Murata K, Mizuguchi Y and Takano Y 2009 Precise pressure dependence of the superconducting transition temperature of FeSe: resistivity and ^{77}Se-NMR study *J. Phys. Soc. Japan* **78** 063704

[155] Tissen V G, Ponyatovsky E G, Nefedova M V, Titov A N and Fedorenko V V 2009 Effects of pressure-induced phase transitions on superconductivity in single-crystal $Fe_{1.02}Se$ *Phys. Rev.* B **80** 092507

[156] Mizuguchi Y, Tomioka F, Tsuda S, Yamaguchi T and Takano Y 2008 Superconductivity at 27 K in tetragonal FeSe under high pressure *Appl. Phys. Lett.* **93** 152505

[157] Miyoshi K, Takaichi Y, Mutou E, Fujiwara K and Takeuchi J 2009 Anomalous pressure dependence of the superconducting transition temperature in $FeSe_{1-x}$ studied by DC magnetic measurements *J. Phys. Soc. Japan* **78** 093703

[158] Horigane K, Takeshita N, Lee C-H, Hiraka H and Yamada K 2009 First investigation of pressure effects on transition from superconductive to metallic phase in $FeSe_{0.5}Te_{0.5}$ *J. Phys. Soc. Japan* **78** 063705

[159] Mizuguchi Y, Tomioka F, Deguchi K, Tsuda S, Yamaguchi T and Takano Y 2010 Pressure effects on FeSe family superconductors *Physica* C **470** S353

[160] Mizuguchi Y, Hara Y, Deguchi K, Tsuda S, Yamaguchi T, Takeda K, Kotegawa H, Tou H and Takano Y 2010 Anion height dependence of T_c for the Fe-based superconductor *Supercond. Sci. Technol.* **23** 054013

[161] Gresty N C *et al* 2009 Structural phase transitions and superconductivity in $Fe_{1+\delta}Se_{0.57}Te_{0.43}$ at ambient and elevated pressures *J. Am. Chem. Soc.* **131** 16944

[162] Okada H, Takahashi H, Mizuguchi Y, Takano Y and Takahashi H 2009 Successive phase transitions under high pressure in $FeTe_{0.92}$ *J. Phys. Soc. Japan* **78** 083709

[163] Zhang C *et al* 2009 Pressure-induced lattice collapse in the tetragonal phase of single-crystalline $Fe_{1.05}Te$ *Phys. Rev.* B **80** 144519

[164] Han Y, Li W Y, Cao L X, Wang X Y, Xu B, Zhao B R, Guo Y Q and Yang J L 2010 Superconductivity in iron telluride thin films under tensile stress *Phys. Rev. Lett.* **104** 017003

[165] Thomas E L, Wong-Ng W, Phelan D and Millican J N 2009 Thermopower of Co-doped FeSe *J. Appl. Phys.* **105** 073906

[166] Williams A J, McQueen T M, Ksenofontov V, Felser C and Cava R J 2009 The metal-insulator transition in $Fe_{1.01-x}Cu_xSe$ *J. Phys.: Condens. Matter* **21** 305701

[167] Huang T-W *et al* 2009 Doping-driven structural phase transition and loss of superconductivity in $M_xFe_{1-x}Se_\delta$ (M = Mn, Cu) *Phys. Rev.* B **82** 104502

[168] Zhang S B, Lei H C, Zhu X D, Li G, Wang B S, Li L J, Zhu X B, Song W H, Yang Z R and Sun Y P 2009 Divergency of SDW and structure transition in $Fe_{1-x}Ni_xSe_{0.82}$ superconductors *Physica* C **469** 1958

[169] Gawryluk D J, Fink-Finowicki J, Wisniewski A, Puzniak R, Domukhovski V, Diduszko R, Kozlowski M and Berkowski M 2011 Growth conditions, structure and superconductivity of pure and metal-doped $FeTe_{1-x}Se_x$ single crystals *Supercond. Sci. Technol.* **24** 065011

[170] Shipra R, Takeya H, Hirata K and Sundaresan A 2010 Effects of Ni and Co doping on the physical properties of tetragonal $FeSe_{0.5}Te_{0.5}$ superconductor *Physica* C **470** 528

[171] Zajdel P, Zubko M, Kusz J and Green M A 2010 Single crystal growth and structural properties of iron telluride doped with nickel *Cryst. Res. Technol.* **45** 1316

[172] Zeng B, Shen B, Chen G F, He J B, Wang D M, Li C H and Wen H H 2011 Nodeless superconductivity of single-crystalline $K_xFe_{2-y}Se_2$ revealed by the low-temperature specific heat *Phys. Rev.* B **83** 144511

[173] Hu R, Cho K, Kim H, Hodovanets H, Straszheim W E, Tanatar M A, Prozorov R, Bud'ko S L and Canfield P C 2011 Anisotropic magnetism, resistivity, London penetration depth and magneto-optical imaging of superconducting $K_{0.86}Fe_{1.84}Se_2$ single crystals *Supercond. Sci. Technol.* **24** 065006

[174] Li Z, Ma X, Pang H and Li F 2011 Evidence of spin excitation gap in $K_{0.86}Fe_{1.73}Se_2$ superconductor as revealed by Mössbauer spectroscopy arXiv:1103.0098

[175] Torchetti D A, Fu M, Christensen D C, Nelson K J, Imai T, Lei H C and Petrovic C 2011 ^{77}Se NMR investigation of the $K_xFe_{2-y}Se_2$ high-T_c superconductor ($T_c = 33$ K) *Phys. Rev.* B **83** 104508

[176] Yuan R H, Dong T, Chen G F, He J B, Wang D M and Wang N L 2011 Nanoscale stripe-type phase separation of antiferromagnetic order and superconductivity in $K_{0.75}Fe_{1.75}Se_2$ arXiv:1102.1381

[177] Mun E D, Altarawneh M M, Mielke C H, Zapf V S, Hu R, Bud'ko S L and Canfield P C 2011 Anisotropic H_{c2} of $K_{0.8}Fe_{1.76}Se_2$ determined up to 60 T *Phys. Rev.* B **83** 100514

[178] Kotegawa H, Hara Y, Nohara H, Tou H, Mizuguchi Y, Takeya H and Takano Y 2011 Possible superconducting symmetry and magnetic correlations in $K_{0.8}Fe_2Se_2$: a ^{77}Se-NMR study *J. Phys. Soc. Japan* **80** 043708

[179] Pomjakushin V Yu, Pomjakushina E V, Krzton-Maziopa A, Conder K and Shermadini Z 2011 Room temperature antiferromagnetic order in superconducting $X_yFe_{2-x}Se_2$, (X = Rb, K): a neutron powder diffraction study *J. Phys.: Condens. Matter* **23** 156003

[180] Luo X G *et al* 2011 Crystal structure, physical properties and superconductivity in $A_xFe_2Se_2$ single crystals *New J. Phys.* **13** 053011

[181] Seyfarth G, Jaccard D, Pedrazzini P, Krzton-Maziopa A, Pomjakushina E, Conder K and Shermadini Z 2011 Pressure cycle of superconducting $Cs_{0.8}Fe_2Se_2$: a transport study *Solid State Commun.* **151** 747

[182] Pomjakushin V Yu, Sheptyakov D V, Pomjakushina E V, Krzton-Maziopa A, Conder K, Chernyshov D, Svitlyk V and Shermadini Z 2011 Iron-vacancy superstructure and possible room-temperature antiferromagnetic order in superconducting $Cs_yFe_{2-x}Se_2$ *Phys. Rev.* B **83** 144410

[183] Liu R H *et al* 2011 Coexistence of superconductivity and antiferromagnetism in single crystals $A_{0.8}Fe_{2-y}Se_2$ (A = K, Rb, Cs, Tl/K and Tl/Rb): evidence from magnetization and resistivity *Europhys. Lett.* **94** 27008

[184] Shermadini Z *et al* 2011 Coexistence of magnetism and superconductivity in the iron-based compound $Cs_{0.8}(FeSe_{0.98})_2$ *Phys. Rev. Lett.* **106** 117602

[185] Lei H, Wang K, Warren J B and Petrovic C 2011 Magnetic and superconducting phase diagram of $K_xFe_{2-y}Se_{2-z}S_z$ ($0 \leqslant z \leqslant 2$) arXiv:1102.2434

[186] Li L, Yang Z R, Zhang Z T, Tong W, Zhang C J, Tan S and Zhang Y H 2011 Coexistence of superconductivity and magnetism in $K_{0.8}Fe_2Se_{1.4}S_{0.4}$ arXiv:1101.5327

[187] Zhou T, Chen X, Guo J, Wang G, Lai X, Wang S, Jin S and Zhu K 2011 Quenching of superconductivity by Co doping in $K_{0.8}Fe_2Se_2$ arXiv:1102.3506

[188] Bao W, Huang Q, Chen G F, Green M A, Wang D M, He J B, Wang X Q and Qiu Y 2011 A novel large moment antiferromagnetic order in $K_{0.8}Fe_{1.6}Se_2$ superconductor *Chin. Phys. Lett.* **28** 086104

[189] Wang K, Lei H and Petrovic C 2011 Thermoelectric studies of $K_xFe_{2-y}Se_2$ indicating a weakly correlated superconductor *Phys. Rev.* B **83** 174503

[190] Li C-H, Shen B, Han F, Zhu X and Wen H-H 2011 Transport properties and anisotropy of $Rb_{1-x}Fe_{2-y}Se_2$ single crystals 2011 *Phys. Rev.* B **83** 184521

[191] Ryan D H, Rowan-Weetaluktuk W N, Cadogan J M, Hu R, Straszheim W E, Bud'ko S L and Canfield P C 2011 ^{57}Fe Mössbauer study of magnetic ordering in superconducting $K_{0.80}Fe_{1.76}Se_{2.00}$ single crystals *Phys. Rev.* B **83** 104526

[192] Ying J J *et al* 2011 Pressure effect on superconductivity of $A_xFe_2Se_2$ (A = K and Cs) *New J. Phys.* **13** 033008

[193] Mou D X *et al* 2011 Distinct Fermi surface topology and nodeless superconducting gap in $(Tl_{0.58}Rb_{0.42})Fe_{1.72}Se_2$ superconductor *Phys. Rev. Lett.* **106** 107001

[194] Guo J, Chen X, Wang G, Zhou T, Lai X, Jin S, Wang S and Zhu K 2011 Superconductivity on the verge of Mott localization in ternary iron sulfide arXiv:1102.3505

[195] Wang X-P, Qian T, Richard P, Zhang P, Dong J, Wang H-D, Dong C-H, Fang M-H and Ding H 2011 Strong nodeless pairing on separate electron Fermi surface sheets in $(Tl,K)Fe_{1.78}Se_2$ probed by ARPES *Europhys. Lett.* **93** 57001

[196] Ma L, Ji G F, Zhang J, He J B, Wang D M, Chen G F, Bao W and Yu W 2011 Superconducting and normal-state properties of single-crystalline $Tl_{0.47}Rb_{0.34}Fe_{1.63}Se_2$ as seen via ^{77}Se and ^{87}Rb NMR *Phys. Rev.* B **83** 174510

[197] Kawasaki Y, Mizuguchi Y, Deguchi K, Watanabe T, Ozaki T, Tsuda S, Yamaguchi T, Takeya H and Takano Y 2011 Pressure study of the new iron-based superconductor $K_{0.8}Fe_2Se_2$ arXiv:1101.0896

[198] Guo J, Sun L, Zhang C, Guo J, Chen X, Wu Q, Gu D, Gao P, Dai X and Zhao Z 2011 Correlation between superconductivity and resistance hump in $K_{0.8}Fe_{1.7}Se_2$ single crystal under high pressure arXiv:1101.0092

[199] Yan X-W, Gao M, Lu Z-Y and Xiang T 2011 Electronic structures and magnetic order of ordered-Fe-vacancy ternary iron selenides $TlFe_{1.5}Se_2$ and $AFe_{1.5}Se_2$ (A = K, Rb, or Cs) *Phys. Rev. Lett.* **106** 087005

[200] Yan X-W, Gao M, Lu Z-Y and Xiang T 2011 Ternary iron selenide $K_{0.8}Fe_{1.6}Se_2$ is an antiferromagnetic semiconductor *Phys. Rev.* B **83** 233205

[201] Shein I R and Ivanovskii A L 2011 Electronic structure and Fermi surface of new K intercalated iron selenide superconductor $K_xFe_2Se_2$ *Phys. Lett.* A **375** 1028

[202] Nekrasov I A and Sadovskii M V 2011 Electronic structure, topological phase transitions and superconductivity in $(K,Cs)_xFe_2Se_2$ *Pis. Zh. Eksp. Teor. Fiz.* **93** 182

[203] Chao C and Jian-Hui D 2011 Electronic structure of KFe_2Se_2 from first principles calculations *Chin. Phys. Lett.* **28** 057402

[204] Cao C and Dai J 2011 Electronic structure and Mott localization of iron-deficient $TlFe_{1.5}Se_2$ with superstructures *Phys. Rev.* B **83** 193104

[205] Zhang Y *et al* 2011 Nodeless superconducting gap in $A_xFe_2Se_2$ (A = K, Cs) revealed by angle-resolved photoemission spectroscopy *Nature Mater.* **10** 273

[206] Qian T *et al* 2011 Absence of holelike Fermi surface in superconducting $K_{0.8}Fe_{1.7}Se_2$ revealed by angle-resolved photoemission spectroscopy *Phys. Rev. Lett.* **106** 187001

[207] Zhao L *et al* 2011 Common Fermi surface topology and nodeless superconducting gap in $K_{0.68}Fe_{1.79}Se_2$ and $(Tl_{0.45}K_{0.34})Fe_{1.84}Se_2$ superconductors revealed from angle-resolved photoemission spectroscopy *Phys. Rev.* B **83** 140508

[208] Maier T A, Graser S, Hirschfeld P J and Scalapino D J 2011 d-wave pairing from spin fluctuations in the $K_xFe_{2-y}Se_2$ superconductors *Phys. Rev.* B **83** 100515

[209] Mazin I I and Schmalian J 2009 Pairing symmetry and pairing state in ferropnictides: theoretical overview *Physica* C **469** 614

[210] Wang F, Yang F, Gao M, Lu Z-Y, Xiang T and Lee D-H 2011 The electron pairing of $K_xFe_{2-y}Se_2$ *Europhys. Lett.* **93** 57003

[211] Zhou Y, Xu D-H, Zhang F-C and Chen W-Q 2011 Theory for superconductivity in $(Tl,K)Fe_xSe_2$ as a doped Mott insulator *Europhys. Lett.* **95** 17003

[212] You Y-Z, Yang F, Kou S-P and Weng Z-Y 2011 Phase diagram and a possible unified description of intercalated iron selenide superconductors arXiv:1103.1902

[213] Saito T, Onari S and Kontani H 2011 Emergence of fully gapped s_{++}-wave and nodal d-wave states mediated by

orbital and spin fluctuations in a ten-orbital model of KFe_2Se_2 *Phys. Rev.* B **83** 140512
[214] Yu W, Ma L, He J B, Wang D M, Xia T-L, Chen G F and Bao W 2011 ^{77}Se NMR study of the pairing symmetry and the spin dynamics in $K_yFe_{2-x}Se_2$ *Phys. Rev. Lett.* **106** 197001
[215] Han F, Shen B, Wang Z-Y and Wen H-H 2011 Reversibly tuning the insulating and superconducting state in $K_xFe_{2-y}Se_2$ crystals by post-annealing arXiv:1103.1347
[216] Bao W, Li G N, Huang Q, Chen G F, He J B, Green M A, Qiu Y, Wang D M and Luo J L 2011 Vacancy tuned magnetic high-T_c superconductor $K_xFe_{2-x/2}Se_2$ arXiv:1102.3674
[217] Yu R, Zhu J-X and Si Q 2011 Mott transition in modulated lattices and parent insulator of $(K,Tl)_yFe_xSe_2$ superconductors *Phys. Rev. Lett.* **106** 186401
[218] Fang C, Xu B, Dai P, Xiang T and Hu J 2011 Magnetic frustration and iron-vacancy ordering in iron-chalcogenide arXiv:1103.4599
[219] Subedi A, Zhang L, Singh D J and Du M-H 2008 Density functional study of FeS, FeSe and FeTe: electronic structure, magnetism, phonons and superconductivity *Phys. Rev.* B **78** 134514
[220] Xia Y, Qian D, Wray L, Hsieh D, Chen G F, Luo J L, Wang N L and Hasan M Z 2009 Fermi surface topology and low-lying quasiparticle dynamics of parent $Fe_{1+x}Te/Se$ superconductor *Phys. Rev. Lett.* **103** 037002
[221] Nakayama K *et al* 2010 Angle-resolved photoemission spectroscopy of the iron-chalcogenide superconductor $Fe_{1.03}Te_{0.7}Se_{0.3}$: strong coupling behavior and the universality of interband scattering *Phys. Rev. Lett.* **105** 197001
[222] Fruchart D, Convert P, Wolfers P, Madar R, Senateur J P and Fruchart R 1975 Structure antiferromagnetique de $Fe_{1.125}Te$ accompagnee d'une deformation monoclinique *Mater. Res. Bull.* **10** 169
[223] Balatsky A V and Parker D 2009 Not all iron superconductors are the same *Physics* **2** 59
[224] Han M J and Savrasov S Y 2009 Doping driven $(\pi, 0)$ nesting and magnetic properties of $Fe_{1+x}Te$ superconductors *Phys. Rev. Lett.* **103** 067001
[225] Ma F, Ji W, Hu J, Lu Z-Y and Xiang T 2009 First-principles calculations of the electronic structure of tetragonal α-FeTe and α-FeSe crystals: evidence for a bicollinear antiferromagnetic order *Phys. Rev. Lett.* **102** 177003
[226] Turner A M, Wang F and Vishwanath A 2009 Kinetic magnetism and orbital order in iron telluride *Phys. Rev.* B **80** 224504
[227] Fang C, Bernevig B A and Hu J 2009 Theory of magnetic order in $Fe_{1+y}Te_{1-x}Se_x$ *Europhys. Lett.* **86** 67005
[228] Moon C-Y and Choi H-J 2010 Chalcogen-height dependent magnetic interactions and magnetic order switching in $FeSe_xTe_{1-x}$ *Phys. Rev. Lett.* **104** 057003
[229] Zaliznyak I A, Xu Z, Tranquada J M, Gu G, Tsvelik A M and Stone M B 2011 Unconventional temperature enhanced magnetism in iron telluride arXiv:1103.5073
[230] Imai T, Ahilan K, Ning F L, McQueen T M and Cava R J 2009 Why does undoped FeSe become a high T_c superconductor under pressure? *Phys. Rev. Lett.* **102** 177005
[231] Bendele M, Amato A, Conder K, Elender M, Keller H, Klauss H-H, Luetkens H, Pomjakushina E, Raselli A and Khasanov R 2010 Pressure induced static magnetic order in superconducting $FeSe_{1-x}$ *Phys. Rev. Lett.* **104** 087003
[232] Sabrowsky H, Rosenberg M, Welz D, Deppe P and Schäfer W 1986 A neutron and Mössbauer study of $TlFe_xS_2$ compounds *J. Magn. Magn. Mater.* **54-57** 1497
[233] Hägström L, Seidel A and Berger R 1991 A Mössbauer study of antiferromagnetic ordering in iron deficient $TlFe_{2-x}Se_2$ *J. Magn. Magn. Mater.* **98** 37
[234] Bacsa J, Ganin A Y, Takabayashi Y, Christensen K E, Prassides K, Rosseinsky M J and Claridge J B 2011 Cation vacancy order in the $K_{0.8+x}Fe_{1.6-y}Se_2$ system: five-fold cell expansion accommodates 20% tetrahedral vacancies *Chem. Sci.* **2** 1054
[235] Cao C and Dai J 2011 Block spin ground state and 3-dimensionality of $(K,Tl)Fe_{1.6}Se_2$ *Phys. Rev. Lett.* submitted (arXiv:1102.1344)
[236] Ye F, Chi S, Bao W, Wang X F, Ying J J, Chen X H, Wang H D, Dong C H and Fang M 2011 Common structural and magnetic framework in the $A_2Fe_4Se_5$ superconductors arXiv:1102.2882
[237] Shen B, Zeng B, Chen G F, He J B, Wang D M, Yang H and Wen H H 2011 Intrinsic percolative superconductivity in $K_xFe_{2-y}Se_2$ single crystals arXiv:1104.2008
[238] Ricci A *et al* 2011 Direct evidence of nanoscale phase separation in the iron chalcogenide superconductor K0.8Fe1.6Se2 from scanning nanofocused x-ray diffraction arXiv:1107.0412
[239] Ricci A *et al* 2011 Intrinsic phase separation in superconducting $K_{0.8}Fe_{1.6}Se_2$ ($T_c = 31.8$ K) single crystals *Supercond. Sci. Technol.* **24** 082002
[240] Maier T A and Scalapino D J 2008 Theory of neutron scattering as a probe of the superconducting gap in the iron pnictides *Phys. Rev.* B **78** 020514(R)
[241] Maier T A, Graser S, Scalapino D J and Hirschfeld P 2009 Neutron scattering resonance and the iron-pnictide superconducting gap *Phys. Rev.* B **79** 134520
[242] Demler E and Zhang S-C 1995 Theory of the resonant neutron scattering of high-T_c superconductors *Phys. Rev. Lett.* **75** 4126
[243] Batista C D, Ortiz G and Balatsky A V 2001 Unified description of the resonance peak and incommensuration in high-T_c superconductors *Phys. Rev.* B **64** 172508
[244] Argyriou D N *et al* 2010 Incommensurate itinerant antiferromagnetic excitations and spin resonance in the $FeTe_{0.6}Se_{0.4}$ superconductor *Phys. Rev.* B **81** 220503
[245] Li S *et al* 2010 Normal-state hourglass dispersion of the spin excitations in $FeSe_xTe_{1-x}$ *Phys. Rev. Lett.* **105** 157002
[246] Babkevich P, Bendele M, Boothroyd A T, Conder K, Gvasaliya S N, Khasanov R, Pomjakushina E and Roessli B 2010 Magnetic excitations of $Fe_{1+y}Se_xTe_{1-x}$ in magnetic and superconductive phases *J. Phys.: Condens. Matter* **22** 142202
[247] Lumsden M S *et al* 2010 Evolution of spin excitations into the superconducting state in $FeTe_{1-x}Se_x$ *Nature Phys.* **6** 182
[248] Diallo S O *et al* 2009 Itinerant magnetic excitations in antiferromagnetic $CaFe_2As_2$ *Phys. Rev. Lett.* **102** 187206
[249] Zhao J, Adroja D T, Yao D-X, Bewley R, Li S, Wang X F, Wu G, Chen X H, Hu J and Dai P 2009 Spin waves and magnetic exchange interactions in $CaFe_2As_2$ *Nature Phys.* **5** 965
[250] Dai P *et al* 2000 Resonance as a measure of pairing correlations in the high-T_c superconductor YBCO *Nature* **406**
[251] Tranquada J M, Lee C H, Yamada K, Lee Y S, Regnault L P and Rønnow H M 2004 Evidence for an incommensurate magnetic resonance in $La_{2-x}Sr_xCuO_4$ *Phys. Rev.* B **69** 174507
[252] Zhao J, Regnault L-P, Zhang C, Wang M, Li Z, Zhou F, Zhao Z, Fang C, Hu J and Dai P 2010 Neutron spin resonance as a probe of the superconducting energy gap of $BaFe_{1.9}Ni_{0.1}As_2$ superconductors *Phys. Rev.* B **81** 180505
[253] Bourges Ph, Keimer B, Pailhòes S, Regnault L P, Sidis Y and Ulrich C 2005 The resonant magnetic mode: a common feature of high-T_c superconductors *Physica* C **424** 45

[254] Bao W, Savici A T, Granroth G E, Broholm C, Habicht K, Qiu Y, Hu J, Liu t and Mao Z Q 2010 A triplet resonance in superconducting $FeSe_{0.4}Te_{0.6}$ arXiv:1002.1617

[255] Li S, Lu X, Wang M, Luo H-q, Wang M, Zhang C, Faulhaber E, Regnault L-P, Singh D and Dai P 2011 Effect of the in-plane magnetic field on the neutron spin resonance in optimally doped $FeSe_{0.4}Te_{0.6}$ and $BaFe_{1.9}Ni_{0.1}As_2$ superconductors *Phys. Rev.* B **84** 024518

[256] Lipscombe O J, Chen G F, Fang C, Perring T G, Abernathy D L, Christianson A D, Egami T, Wang N, Hu J and Dai P 2011 Spin waves in the $(\pi, 0)$ magnetically ordered iron chalcogenide $Fe_{1.05}Te$ *Phys. Rev. Lett.* **106** 057004

[257] Stock C, Rodriguez E E, Green M A and Rodriguez-Rivera J A 2011 Interstitial iron tuning on the spin fluctuations in the nonsuperconducting parent phase $Fe_{1+x}Te$ *Phys. Rev.* B **84** 045124

[258] Xu Z, Wen J, Xu G, Chi S, Ku W, Gu G and Tranquada J M 2011 Local-moment magnetism in superconducting $FeTe_{0.35}Se_{0.65}$ as seen via inelastic neutron scattering *Phys. Rev.* B **84** 052506

[259] Wang M *et al* 2010 Spin waves and magnetic exchange interactions in insulating $Rb_{0.89}Fe_{1.58}Se_2$ arXiv:1105.4675